ResearchGate

See discussions, stats, and author profiles for this publication at: https://www.researchgate.net/publication/46821468

Geological constraints on the origin of oxygenic photosynthesis. Photosynth Res

ARTICLE *in* PHOTOSYNTHESIS RESEARCH · SEPTEMBER 2010

Impact Factor: 3.5 · DOI: 10.1007/s11120-010-9594-0 · Source: PubMed

CITATIONS
108

READS
45

3 AUTHORS, INCLUDING:

James Farquhar
University of Maryland, College Park

131 PUBLICATIONS **5,314** CITATIONS

SEE PROFILE

Andrey Bekker
University of California, Riverside

150 PUBLICATIONS **4,291** CITATIONS

SEE PROFILE

All in-text references underlined in blue are linked to publications on ResearchGate, letting you access and read them immediately.

Available from: Andrey Bekker
Retrieved on: 24 January 2016

Geological constraints on the origin of oxygenic photosynthesis

Photosynthesis Research
Official Journal of the
International Society of
Photosynthesis Research

ISSN 0166-8595
Volume 107
Number 1

Photosynth Res (2010)
107:11-36
DOI 10.1007/
s11120-010-9594-0

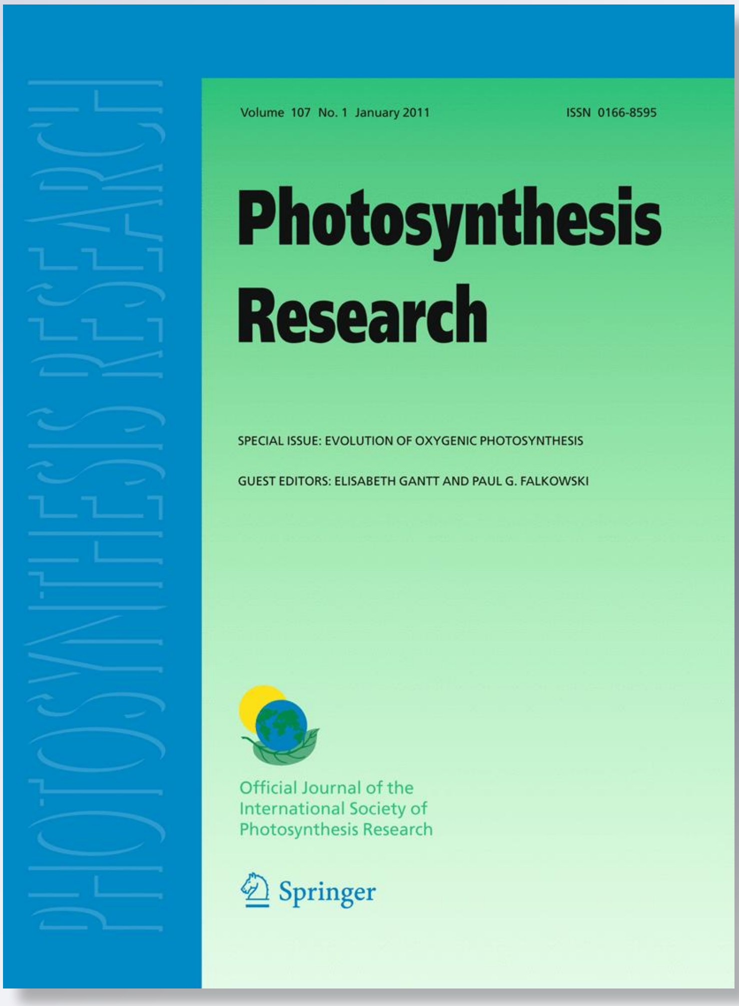

PHOTOSYNTHESIS RESEARCH

Volume 107 No. 1 January 2011 ISSN 0166-8595

Photosynthesis
Research

SPECIAL ISSUE: EVOLUTION OF OXYGENIC PHOTOSYNTHESIS

GUEST EDITORS: ELISABETH GANTT AND PAUL G. FALKOWSKI

Official Journal of the
International Society of
Photosynthesis Research

Springer

Springer

Photosynth Res (2011) 107:11–36
DOI 10.1007/s11120-010-9594-0

REVIEW

Geological constraints on the origin of oxygenic photosynthesis

James Farquhar · Aubrey L. Zerkle ·
Andrey Bekker

Received: 14 October 2009 / Accepted: 18 August 2010 / Published online: 30 September 2010
© Springer Science+Business Media B.V. 2010

Abstract This article examines the geological evidence for the rise of atmospheric oxygen and the origin of oxygenic photosynthesis. The evidence for the rise of atmospheric oxygen places a minimum time constraint before which oxygenic photosynthesis must have developed, and was subsequently established as the primary control on the atmospheric oxygen level. The geological evidence places the global rise of atmospheric oxygen, termed the Great Oxidation Event (GOE), between ~2.45 and ~2.32 Ga, and it is captured within the Duitschland Formation, which shows a transition from mass-independent to mass-dependent sulfur isotope fractionation. The rise of atmospheric oxygen during this interval is closely associated with a number of environmental changes, such as glaciations and intense continental weathering, and led to dramatic changes in the oxidation state of the ocean and the seawater inventory of transition elements. There are other features of the geologic record predating the GOE by as much as 200–300 million years, perhaps extending as far back as the Mesoarchean–Neoarchean boundary at 2.8 Ga, that suggest the presence of low level, transient or local, oxygenation. If verified, these features would not only imply an earlier origin for oxygenic photosynthesis, but also require a mechanism to decouple oxygen production from oxidation of Earth's surface environments. Most hypotheses for the GOE suggest that oxygen production by oxygenic photosynthesis is a precondition for the rise of oxygen, but that a synchronous change in atmospheric oxygen level is not required by the onset of this oxygen source. The potential lag-time in the response of Earth surface environments is related to the way that oxygen sinks, such as reduced Fe and sulfur compounds, respond to oxygen production. Changes in oxygen level imply an imbalance in the sources and sinks for oxygen. Changes in the cycling of oxygen have occurred at various times before and after the GOE, and do not appear to require corresponding changes in the intensity of oxygenic photosynthesis. The available geological constraints for these changes do not, however, disallow a direct role for this metabolism. The geological evidence for early oxygen and hypotheses for the controls on oxygen level are the basis for the interpretation of photosynthetic oxygen production as examined in this review.

Keywords Oxygen evolution · Atmospheric oxygenation · Origin of photosynthesis · Iron speciation · Transition elements · Isotopes · Mass independent · Sulfur isotopes · Nitrogen metabolism

Introduction

Oxygenic photosynthesis is one of the most important biological innovations to have occurred since the appearance of life on our planet. Oxygenic photosynthesis (and respiration) provided a very effective means for production of biomass and energy, and for the diversification of life on an ancient Earth. While definitive evidence for an oxygenated atmosphere and expansion of oxygenic

J. Farquhar (✉) · A. L. Zerkle
Department of Geology and ESSIC, University of Maryland, College Park, MD 20742, USA
e-mail: jfarquha@geol.umd.edu

A. L. Zerkle
e-mail: azerkle@umd.edu

A. Bekker
Department of Geological Sciences, University of Manitoba, Manitoba R3T 2N2, Canada
e-mail: bekker@cc.umanitoba.ca

photosynthesis appears in rocks younger than ~2.45 Ga, some geological evidence may point to an earlier appearance of oxygen and this metabolism. Some of the proposed evidence for an earlier accumulation of oxygen produced via photosynthesis remains controversial.

This review examines the proxies for surface oxidation that define the primary rise of atmospheric oxygen, the Great Oxidation Event—GOE (cf. Holland 2002, 2006). We review the arguments that have been made on the basis of the rock record, the geochemistry of transition elements, and the record of stable isotope variations, for the pervasive oxidation of the Earth's surface environments between 2.45 and 2.32 Ga. This event provides a minimum boundary for the evolution of oxygenic photosynthesis. We also review mounting evidence for transient low levels of oxygen in some environments (also called "whiffs" of oxygen and local oxygen oases) from 100 to 200 million years before the GOE. These events could allow for an earlier origin of oxygenic photosynthesis as early as 2.8 Ga. The records of these earlier events do not always behave in ways similar to those at the time of the GOE or at later times, and alternative explanations for the data have been proposed. We review these observations and discuss the implications for the appearance of oxygenic photosynthesis.

Geological record of banded iron formation

Banded iron formations (BIFs) are marine sedimentary rocks that consist predominantly of iron oxides, silicon dioxide (chert or quartz), iron carbonates (siderite and ankerite), and iron silicates. They can be enormous in scale, extending over hundreds of square kilometers. BIFs are subdivided into two groups, based on their extent, relationship with volcanic formations, and tectonic and depositional setting (Gross 1996). The Algoma-type iron formations are associated with volcanic rocks (normally bimodal in composition, indicating Mg+Fe-rich and Si+Al-rich magmas) and occur in restricted basins in volcanic arc and back-arc settings. This type of iron formation is commonly associated with barren and base metal-rich sulfide deposits and is common in Precambrian as well as in Phanerozoic basins (e.g., Peter et al. 2003). The Superior-type iron formations were developed in a range of water depths on continental shelves within predominantly sedimentary successions (e.g., Planavsky et al. 2009); they cover extensive areas and are not directly associated with volcanic units. The Superior-type iron formations are restricted to the Precambrian, disappearing from the geological record approximately 1.8–1.9 billion years ago and reappearing briefly approximately 700 million years ago (e.g., Bekker et al. 2010). Their presence in the ancient record is taken as evidence for ocean chemistry with dissolved iron that has not existed in the more recent geologic past.

For many (e.g., Cloud 1973; Holland 1973), the presence of Superior-type iron formations has been taken as one of the most important indicators of the evolution of oxygen level in Earth's early oceans, and points to surface environments with oxygen levels that were significantly lower than today. Their presence implies relatively high levels of dissolved ferrous iron in the oceans, and sedimentary fabrics preserved by different Superior-type iron formations point to their formation in both shallow- and deep-water environments. Since soluble iron reacts with oxygen and sulfide to form insoluble minerals (ferric oxides or sulfides), a long-lived ferruginous ocean implies a higher rate of delivery of soluble iron (Fe^{2+}) than of either oxygen (thought to be generated by oxygenic photosynthesis) or sulfide (typically thought to be generated by bacterial sulfate reduction). The presence of Superior-type iron formations during this time does not, however, require an absence of oxygen production by photosynthesis, but it places a direct limit on the amount of oxygen that was present in the ocean. Moreover, since one requirement for sulfate reduction is a ready supply of sulfate by the oxidative continental weathering of sulfide minerals, this provides a secondary tie to the oxidation state of Earth's early environments.

Questions still remain, however, about how the development of Superior-type iron formations is tied to Earth surface oxygenation. The apparent disappearance of Superior-type iron formations from the rock record does not end at the time of the GOE. This type of iron formation persisted 300–400 million years later, ending at approximately 1.8–1.9 Ga, and must therefore respond to the changes in atmospheric oxygen levels in ways that are more complex than simply being tied to the appearance of atmospheric oxygen. It has been suggested that this delay reflects a long-term or transient change in ocean redox state due to a change in the flux of components to the ocean such as sulfate (Canfield 1998), oxygen (Holland 1984; Slack et al. 2007), and hydrothermal iron (Bekker et al. 2010). It has similarly been suggested that the presence of Superior-type iron formations in the Archean and early Proterozoic may reflect special oceanic conditions, when large amounts of hydrothermal iron were introduced into the oceans. This suggestion links the deposition of large iron formations to mantle plume breakout events and formation of large volcanogenic massive sulfide deposits, sea-level rise, and deposition of organic matter-rich sulfidic shales (e.g., Barley et al. 1998; Condie et al. 2001; Bekker et al. 2010) (Fig. 1). These suggestions are partly based on an episodicity of BIF deposition in the Archean and Early Paleoproterozoic that appears to be correlated with inferred

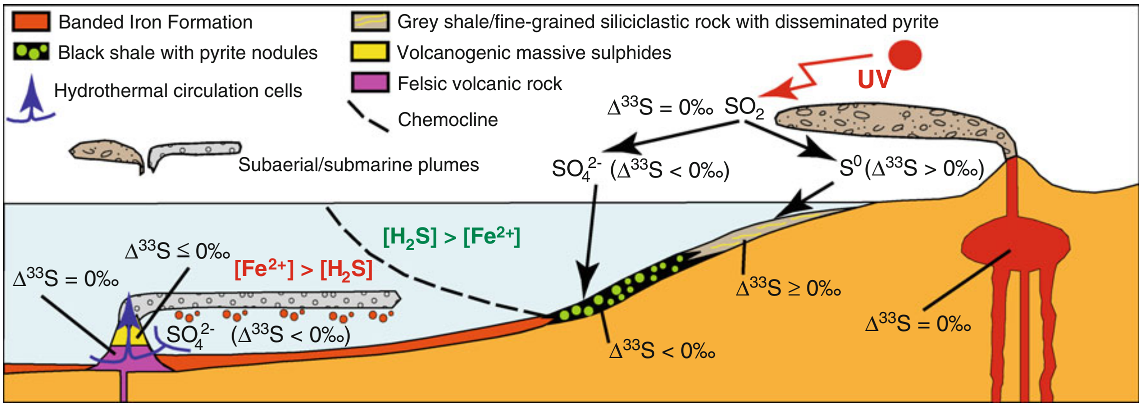
Banded Iron Formation
Black shale with pyrite nodules
Hydrothermal circulation cells
Grey shale/fine-grained siliciclastic rock with disseminated pyrite
Volcanogenic massive sulphides
Felsic volcanic rock
Chemocline
Subaerial/submarine plumes
UV
$\Delta^{33}S = 0‰$ SO_2
SO_4^{2-} ($\Delta^{33}S < 0‰$)
S^0 ($\Delta^{33}S > 0‰$)
$[H_2S] > [Fe^{2+}]$
$\Delta^{33}S \leq 0‰$
$[Fe^{2+}] > [H_2S]$
$\Delta^{33}S = 0‰$
SO_4^{2-} ($\Delta^{33}S < 0‰$)
$\Delta^{33}S \geq 0‰$
$\Delta^{33}S < 0‰$
$\Delta^{33}S = 0‰$

Fig. 1 Schematic diagram illustrating multiple sulfur isotope composition of depositional environments influenced by mass-independent sulfur isotope fractionations in the Archean anoxic atmosphere during the major Archean mantle plume breakout events (modified from Bekker et al. 2009). Note that sulfur was supplied to the atmosphere by subaerial volcanism at the same time as iron was delivered to the ocean by submarine hydrothermal processes during the times when large igneous provinces were formed. It is conceivable that under these conditions a dynamic chemocline would develop in the ocean with shallow-water continental slope settings having larger sulfur than iron flux, whereas the deep ocean would be dominated by hydrothermal iron flux. Geological cross-sections through well preserved Archean basins support this facies arrangement and iron isotope data (e.g., Rouxel et al. 2005) are also consistent with this interpretation

global-scale tectonic events. The last of the Paleoproterozoic Superior-type iron formations occurred at 1.88 Ga and coincides with a time when a supercontinent was assembled, extensive arc environments existed, and when mantle plume breakout events affected North America and other continents (e.g., Heaman et al. 2009; Planavsky et al. 2009). While these suggestions have linked the presence of Superior-type iron formation in the geologic record to ocean redox state and hydrothermal iron flux, links to atmospheric oxygen are still indirectly implied by their presence, since seawater oxygen and sulfate levels, linked to atmospheric composition and oxidative weathering, are considered to play a controlling role in iron transport from the deep ocean.

Other lithological indicators of oxygenation

A number of other geological observations also suggest a dramatic difference between the oxidation state of the Earth before the GOE when compared to that of more recent times (Fig. 2). Geological evidence suggesting a change in the redox state of the oceans and atmosphere near the time of the GOE includes:

- Red beds, iron oxide-bearing sedimentary rocks which form in dry oxidized terrestrial fluvial environments, first appeared around 2.3 Ga in Canada and Fennoscandia (Chandler 1980; Melezhik et al. 2005).
- Sediment-hosted Stratiform Copper Deposits, which form in preexisting sediments by leaching of proximal volcanics with hypersaline (high salinity) oxidized fluids, also first appeared around 2.25 Ga (Kirkham and Roscoe 1993).
- Well-rounded pebbles of the minerals uraninite (UO_2), pyrite (FeS_2), and siderite ($FeCO_3$), which are unstable in modern oxidized fluvial environments, are common only in conglomerates deposited in fluvial and shallow-marine settings before ~2.3 Ga (Rasmussen and Buick 1999; Roscoe 1996; England et al. 2002; Hofmann et al. 2009).
- Paleosols, ancient weathering horizons that form in contact with the atmosphere, are leached of iron when older than ~2.4 Ga because Fe^{2+} is soluble but retained iron when younger than ~2.22 Ga because Fe^{3+} occurs as insoluble oxy(hydr)oxides (e.g., Rye and Holland 1998).
- Sulfate evaporites with evidence of sulfate precipitating before halite are only reported in shallow-marine settings younger than the GOE (Schröder et al. 2008; Pope and Grotzinger 2003; Grotzinger and Kasting 1993), this sequence of precipitation implies an increase in seawater sulfate concentrations after the rise of atmospheric oxygen.
- Extensive manganese deposits, phosphorites, and glauconite, all of which directly or indirectly depend on oxic ocean conditions, first appear after the GOE (Holland 2005; Melezhik et al. 2005; Wood 1973). The Mn deposits in the 2.22 Ga Hotazel Fm. are the oldest, large (in thickness and geographic extent) unambiguous Mn-oxide deposits and contain a prominent negative Ce anomaly indicating that shallow-marine environments by that time were oxygenated (Tsikos and Moore 1997).

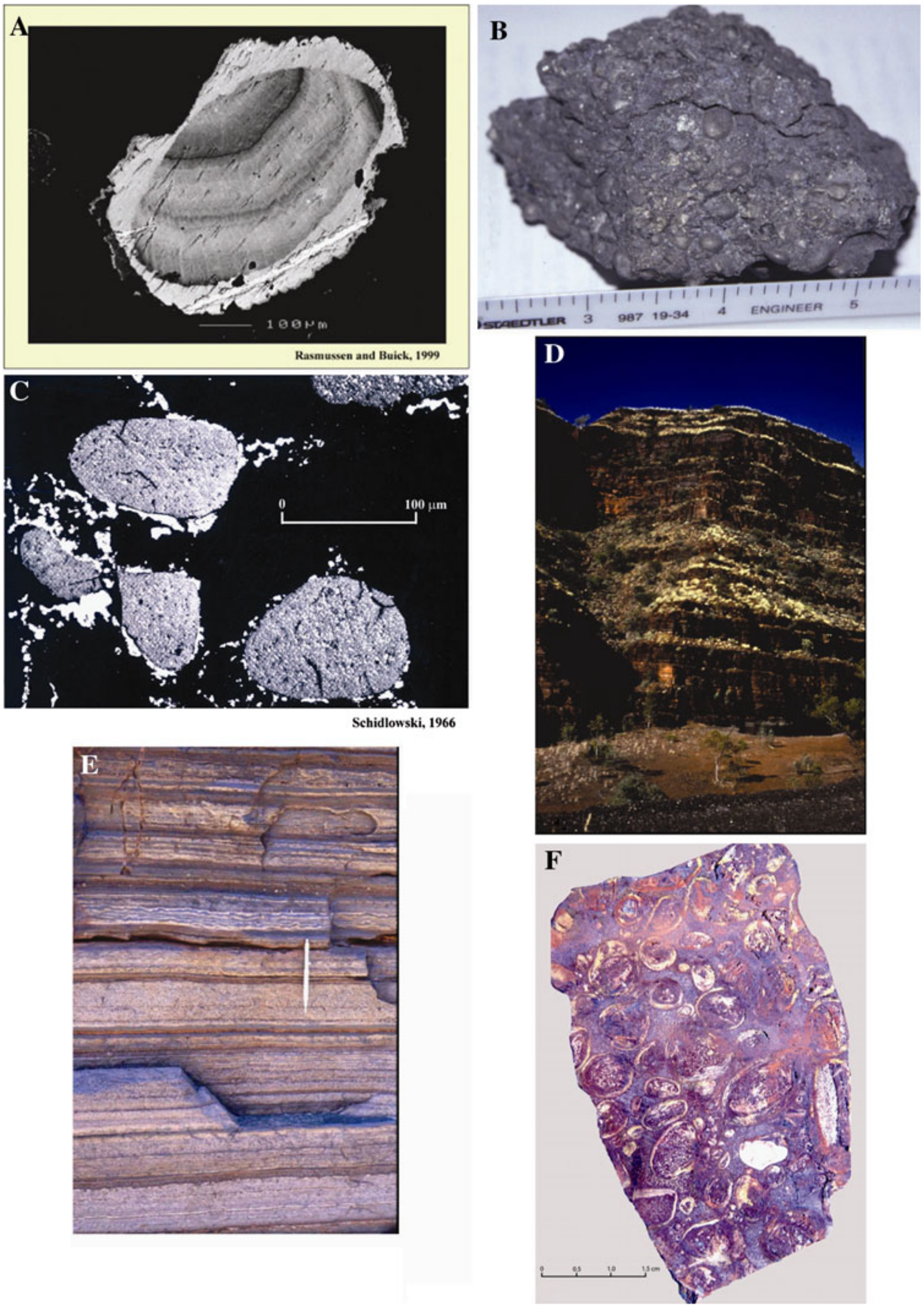

Fig. 2 Redox indicators for the ancient atmosphere and ocean and proxies for environmental changes during the early Paleoproterozoic (2.5–2.0 Ga). **a** Rounded detrital siderite grain from fluvial sandstones of the ~2.7 Ga Fortescue Group, Western Australia (modified from Rasmussen and Buick 1999); **b** rounded pyrite grains from the fluvial to shallow-marine ~2.64 Ga Black Reef Quartzite Formation, South Africa (see Hofmann et al. 2009); **c** detrital uraninite grain from the ~2.9 Ga Witwatersrand Group, South Africa (modified from Schidlowski 1966); **d** ~2.47 Ga Dales Gorge Member, Brockman Iron Formation of Western Australia; **e** banded iron formation from the ~2.47 Ga Dales Gorge Member, Brockman Iron Formation of Western Australia; **f** ~2.30 Ga granular iron formation in the Timeball Hill Formation of South Africa; **g** glacial dropstone in the finely laminated shale of the ~2.3 Ga Gowganda Formation, Canada; **h** cross-bedded red beds in the upper part of the ~2.3 Ga Gowganda Formation in Canada; **i** mature quartz sandstone above the youngest Paleoproterozoic glacial diamictite in the Hurwitz Group, Canada (see Aspler et al. 1994); **j** molds of gypsum in red-colored siltstone of the ~2.3–2.2 Ga Kona Dolomite, USA (modified from Bekker et al. 2006); **k** domal stromatolite in dolomites of the ~2.3–2.2 Ga Kona Dolomite, USA (modified from Bekker et al. 2006); and **l** corestones in the weathering horizon (paleosols) developed over the 1.88 Ga mafic volcanics in Flin Flon, Manitoba, Canada

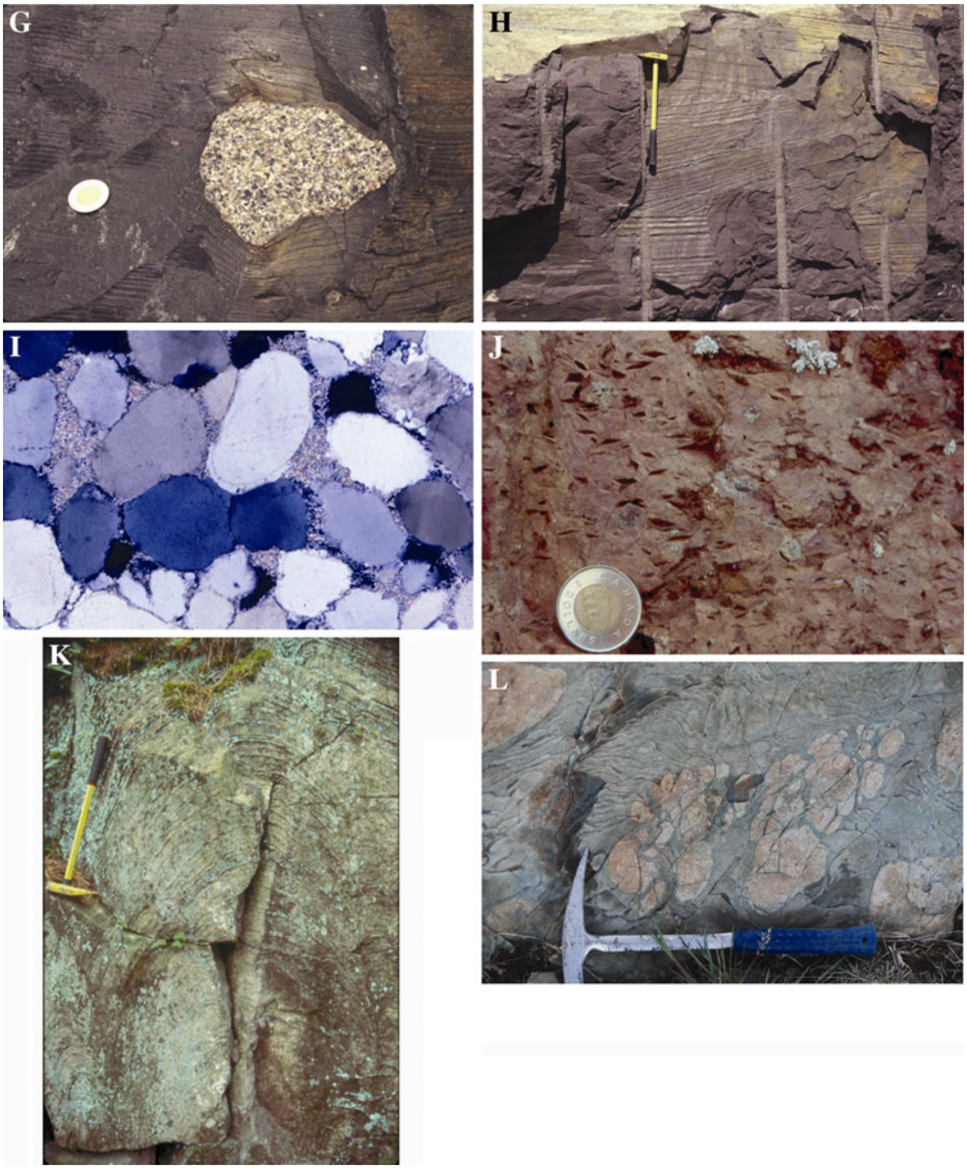

Fig. 2 continued

From a uniformitarian standpoint, oxygen is the common link for all these observations. Oxygen controls these proxies in the modern environment, and their records in ancient environments can be explained by lower atmospheric oxygen levels prior to ~ 2.4 Ga. Geological arguments for a rise of oxygen were first made more than 80 years ago (e.g., MacGregor 1927), and have thereafter formed the basis for assertions that the oxygen content of surface environments and of the atmosphere dramatically changed between approximately 2.45 and 2.22 Ga. The strength of these arguments lies in their compatibility, so that changes in independent proxies are temporally and stratigraphically consistent. This logical consistency has not yet been challenged by any other model that unifies alternative interpretations of all the individual proxies. It also attests to the widespread and profound impact that oxygen production has had on the surface processes on this planet.

Transition element geochemistry

The abundance and speciation of transition elements (columns 3–11 on the periodic table) in sedimentary rocks have also been used to constrain ocean and atmospheric oxygen levels. The abundance of these elements in the oceans depends strongly on the balance between their supply, mostly via weathering, and their sinks, as mainly oxide and sulfide minerals formed in the sediments and in the water column. Oxygen levels in the atmosphere influence the supply of transition elements to the oceans by weathering of silicates, sulfides, and other redox-sensitive minerals (Holland 1984).

The residence time of transition elements in the oceans and their burial efficiency in marine sediments also depends on the oxidation state of seawater, which controls their chemical speciation and the solubility of their various compounds (Holland 1984; Scott et al. 2008). For instance, under oxygen-rich conditions elements like uranium and molybdenum are highly soluble in oxidized form (as UO_2^{2+} and MoO_4^{2-}), in contrast to Fe^{3+} and Mn^{4+}, which readily form insoluble metal (oxyhydr)oxides. The solubility and burial of these elements also depends on the sulfide concentration, because many are chalcophile (bond easily with sulfur), and this leads to an intricate dependence of their chemistry on both oxygen and sulfur.

Of the transition elements, the records of Fe and Mo have yielded the most significant information about oxygen near the time of the GOE. Other transition elements must also have responded to changes in oxygen levels during this time interval, but the state of research on the records of, for instance, Re–Os, Cu, and Ni is less developed than those of Fe and Mo (Yang and Holland 2002; Konhauser et al. 2009; Partin et al. 2010; Kendall et al. 2010). For some of these elements, such as Ni (Konhauser et al. 2009), the connection is inferred to be driven not by oxygen, but by mantle heat dissipation and is instead proposed as a potential driver of changes in the global ecology that may have ultimately fed into oxidation. Below we focus in turn on what has been obtained from the records of Fe and Mo, because these are thought to provide strong ties to the atmosphere and ocean oxidation state and oxygenation events.

Iron speciation

Although evidence for ferruginous oceans (containing appreciable dissolved Fe^{2+}) exists in sequences considerably younger than the time of the GOE, including ~1.8–1.9 Ga extensive Superior-type iron formation deposits, iron chemistry also provides information about the oxidation state of Earth's oceans during and before the GOE. Examination of modern sediments deposited under a range of depositional settings has shown that the speciation of iron in sediments is indicative of the redox state of the overlying water column (Poulton and Raiswell 2002).

Iron speciation is quantified using a number of operationally defined parameters, such as the ratio of highly reactive iron to total iron (FeHR/FeT) and the extent to which the Fe pool has been pyritized (FeP/FeHR). Sediments deposited from anoxic waters commonly have FeHR/FeT greater than 0.38, while sediments deposited under oxygenated waters have ratios significantly below this level (~0.14 for modern sediments; Poulton and Raiswell 2002). In anoxic sediments with FeHR/FeT greater than 0.38, FeP/FeHR values greater than ~0.8 indicate deposition from a sulfidic water column, and FeP/FeHR values less than ~0.8 indicate deposition from a ferruginous water column (Poulton et al. 2004). For these reasons FeHR/FeT and FeP/FeHR have been used to distinguish three different states of water column chemistry: (1) anoxic and ferruginous, (2) anoxic and sulfidic ("euxinic"), and (3) fully oxygenated. Establishment of these conditions depends on the relative fluxes of iron, sulfide, oxygen, and other reductants and oxidants to the water column.

Recent application of Fe speciation to Archean and early Proterozoic successions suggest transiently sulfidic seawater conditions in 2.7–2.5 Ga basins in South Africa and Western Australia (Poulton et al. 2009; Reinhard et al. 2009). This may imply a higher supply of sulfate due to enhanced oxidative weathering followed by microbial sulfate reduction leading to a buildup of sulfide concentrations that overwhelmed the iron dissolved in the water column. This may also imply processes not linked to transient oxygenation if the euxinic conditions were basinal or even facies-restricted in extent rather than a global ocean feature. The condition for euxinia is an excess of sulfide over Fe^{2+} and oxygen, and this could arise in a basinal setting if $[H_2S]/[Fe^{2+}] > \sim 1$, as determined by the stoichiometry of early diagenetic sulfide minerals, mackinawite and greigite. This condition can develop if $[SO_4{:}\ S]/[Fe^{2+}] > \sim 1$ and if microbial sulfate reduction rates determined by local redox conditions were high enough to tip the balance in favor of sulfide over iron.[1] Few applications of Fe-speciation techniques closer to the inferred time of the GOE have been published, other than in abstract form (e.g., Poulton et al. 2009; Reinhard et al. 2009), but these ongoing studies will provide additional constraints on the behavior of iron, sulfur, and oxygen in early environments during this transition, and it is anticipated that a rich record of aqueous iron–sulfur–oxygen chemistry will be revealed.

Molybdenum concentrations in euxinic shales

Molybdenum is another relatively recently developed transition element paleoredox indicator that has been used to study ocean chemistry in the sedimentary units deposited before and after the GOE (Holland 1984, 2003; Algeo and Lyons 2006; Anbar et al. 2007; Scott et al. 2008). Molybdenum is supplied to the oceans primarily by the riverine flux of molybdate (MoO_4^{2-}) derived from the oxidative weathering of sulfide minerals (Bertine and Turekian 1973; Taylor and McLennan 1995; Lyons et al. 2003). Low-temperature hydrothermal systems in the modern ocean constitute ~1/9 of the riverine Mo flux to the ocean (Morford and Emerson 1999; McManus et al. 2002). Although it is a minor flux to the modern ocean, in absence or minor contribution of riverine Mo flux to the Archean ocean Mo reservoir, low-temperature hydrothermal Mo flux might have been quantitatively more important. The molybdate anion is highly conservative, with a long residence time, in today's well-mixed oceans. As a result, molybdenum is the most abundant transition element in the modern oxygenated oceans, at an average concentration of ~100 nM (Bertine and Turekian 1973; Collier 1985). The only significant sink for molybdate in well-oxygenated environments is believed to be co-precipitation and burial with Mn-oxyhydroxides, but this is a very slow process that only removes minor amounts of Mo from the ocean today (Bertine and Turekian 1973). The most significant sinks for Mo in modern environments are in euxinic settings, where molybdate reacts with sulfide to produce particle-reactive thiomolybdates ($MoO_xS_{4-x}^{2-}$) (Helz et al. 1996; Lyons et al. 2003), and removed primarily by sorption onto organic matter. Continental margin settings have also been suggested as an important sink for Mo in the modern oceans (e.g., McManus et al. 2006), related directly to organic carbon burial or indirectly through the coupling of carbon and sulfur burial.

---

[1] We include all sulfur species with sulfate here because of the possibility of their atmospheric contribution to the Archean sulfur cycle.

In modern euxinic environments with a high supply of Mo, such as the Cariaco Basin, the concentration of Mo in the sediments exceeds average crustal values by two orders of magnitude, and elevated ratios of Mo to total organic carbon (Mo/TOC) develop (Lyons et al. 2003; Algeo and Lyons 2006). In settings such as the Black Sea, Mo sinks outpace Mo supply. Low Mo concentrations develop in the water column, and the magnitude of Mo enrichment and Mo/TOC ratios in sediments drop precipitously (Algeo and Lyons 2006). This feature of Mo geochemistry is the basis for the use of Mo concentrations in euxinic black shales as a proxy for seawater Mo and, indirectly, for molybdate delivery to the oceans. The two examples given above (the Cariaco Basin and the Black Sea) highlight an important assumption that is necessary for this approach to work. The sediments utilized in studies of ancient Mo concentration and Mo/TOC ratios should be in communication with the global oceanic Mo pool, because if they reflect restricted basin dynamics or a local source or sink, inferences for the cycling of Mo on a global scale may be invalid. For example, anoxic and sulfidic basins with a higher degree of isolation from the global ocean will develop lower seawater Mo concentrations and, therefore, study of sedimentary rocks deposited in these settings will underestimate seawater Mo inventory in the global ocean.

The Mo and Mo/TOC records for sediments with clear communication with the open ocean do not show evidence for a large oceanic Mo inventory before ~2.15 Ga (Scott et al. 2008), considerably later than most estimates for the timing of the GOE and well after the disappearance of detrital sulfides from the sedimentary rock record (e.g., Roscoe 1996). At least two factors could have contributed to the small seawater Mo inventory in the immediate aftermath of the GOE, if this signal accurately reflects marine Mo levels. First, the ocean redox state may have lagged atmospheric oxidation leading to extensive areas with euxinic, anoxic, and suboxic sinks for Mo. This factor alone might be unable to explain the ~200 Ma delay in response of the seawater Mo inventory, since none of the Phanerozoic euxinic events, regardless of how long they lasted, show similar low Mo-enrichments.

Another factor might be tied to the Mo distribution in the continental crust, as has been argued for Re and Os by Hannah et al. (2004). The present continental flux of Mo, like that of Re and Os, is largely derived from organic matter-rich sulfidic shales; at the time of the GOE, the pre-GOE organic matter-rich sulfidic shales were not significantly enriched in Mo above crustal levels (Holland 2004; Yamaguchi 2002; Scott et al. 2008). The predominant crustal reservoir of Mo that oxidized to form molybdate at this time would have been crystalline crustal rocks with generally low Mo content. This would result in a small supply of Mo to the oceans in the immediate aftermath of the GOE in spite of high supply of species like sulfate. The time for ingrowth of a large reservoir of Mo-enriched shales may have been comparable to the crustal residence time (~200 Ma), and the process would ultimately lead to higher oceanic Mo contents as [Mo] increased in the source rocks (e.g., organic matter-rich, sulfidic shales) that were being weathered.

There also appear to be intervals with small enrichments in Mo over typical baseline Archean levels in the ~2.50–2.65 Ga geologic record leading up to the time of the GOE (Wille et al. 2007; Anbar et al. 2007; Scott et al. 2008); some of which are coincident with inferred euxinic conditions (Scott et al. 2008; Reinhard et al. 2009). These are discussed further below in the section on possible evidence for low-level oxygenation before the GOE.

Stable isotope records

The carbon isotope record

Positive $\delta^{13}C$ excursions in carbonates

Variations in the relative abundances of stable isotopes provide additional constraints on the rise of atmospheric oxygen and the connections with oceanic and atmospheric redox states and the carbon cycle. In particular, the secular trend of $\delta^{13}C$ values in marine carbonates is linked to organic carbon burial and the oxidation of Earth's surface environments associated with the GOE (Karhu and Holland 1996; Bekker and Kaufman 2007; Holland 2009).[2] The striking feature of the carbon isotope record is that the carbon isotope values of carbonates deposited before ~2.4 Ga and between 2.06 and 0.8 Ga fall within a narrow range centered on 0‰. In contrast, there are two or three carbon isotope excursions between 2.4 and 2.06 Ga closely associated with the rise of atmospheric oxygen and Paleoproterozoic climatic changes (Bekker et al. 2006) (Fig. 3). Carbon isotope variations have been interpreted in two ways. It has been suggested that the ^{13}C enrichments reflect an increase in the proportion of ^{13}C-depleted organic matter that was buried (Karhu and Holland 1996). It has also been suggested that the ^{13}C enrichments reflect methanogenesis, with carbonate precipitation influenced by ^{13}C-enriched CO_2 produced in this early diagenetic realm (Hayes and Waldbauer 2006). Karhu and Holland (1996) suggested that high relative burial rate of organic matter between ~2.2 and 2.1 Ga during the Lomagundi carbon isotope excursion led to the rise of atmospheric oxygen. This interpretation has been a focus of recent debate (e.g., Zahnle et al. 2006; Hayes and Waldbauer 2006), because the rise of atmospheric oxygen appears to start before the Lomagundi excursion (Bekker et al. 2004), and because accumulated atmospheric oxygen would not persist on a geologic time scale unless significant amounts of organic matter were permanently isolated from subsequent oxidation, such as the case of deposition on oceanic crust in the deep ocean and subduction to the mantle (Catling et al. 2001). A separate, older carbon isotope excursion in the Duitschland Formation of South Africa (Bekker et al. 2001) is associated with the appearance of mass-dependently fractionated sulfur and follows the disappearance of mass-independently fractionated sulfur (Guo et al. 2009 and discussion below). The nature of this record makes it difficult to speculate with any confidence about a cause-and-effect relationship between burial of organic matter and atmospheric oxidation during this interval. It would appear that the largest positive carbon isotope excursions are a response to atmospheric oxidation rather than a driver for it. Holland (2002) has suggested that such a response may reflect a higher flux of nutrients from the continents in response to the emergence of oxidative, acidic weathering. The evidence for more than one carbon isotope excursion combined with paleoclimatic evidence for several Paleoproterozoic glaciations following the first evidence for an oxygenated atmosphere suggests that this transition was not a simple "on–off" type of event, but involved feedbacks and longer-term system responses, likely involving large reservoirs such as the oceans, and changes in carbon isotope fractionations associated with redox-controlled secondary and primary productivity (Bekker et al. 2008).

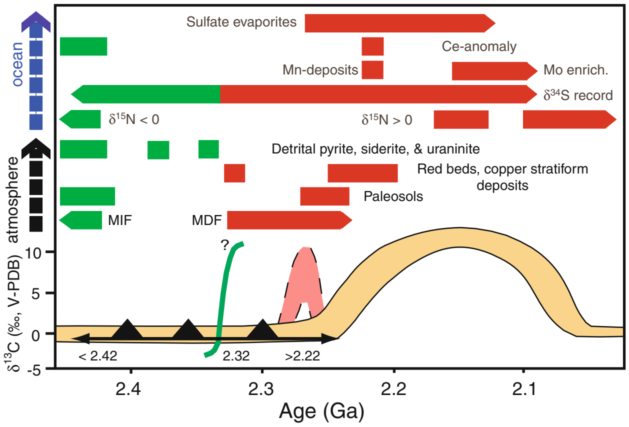

Fig. 3 Schematic representation of Paleoproterozoic secular carbon isotope variations within a framework of other redox indicators discussed here. The *black triangles* represent the three Paleoproterozoic glaciations with their age constraints shown. The Paleoproterozoic glacial epoch is bracketed between 2.42 and 2.22 Ga; 2.32 Ga Re/Os isochrone age of pyrites from black shales deposited before the last glacial event (Hannah et al. 2004) provide another age constraint for these glacial events. *Yellow curve* of secular carbon isotope variations is from Karhu and Holland (1996). *Green curve* represents worldwide recognized negative carbon isotope excursion in cap carbonates above the second Huronian glaciation (Bekker et al. 2005) and positive carbon isotope excursion so far documented only from the Duitschland Formation of South Africa (Bekker et al. 2001). Recently recognized positive carbon isotope excursion in the aftermath of the last Paleoproterozoic ice age and before the Lomagundi excursion is shown in *pink* (cf. Bekker et al. 2006). Indicators for redox state of the atmosphere (*black text*) and ocean (*grey text*) are shown in *green* (reducing) and *red* (oxidized) and are organized in somewhat subjective way from the most sensitive to the oxygen level at the bottom to the least sensitive at the top

Negative $\delta^{13}C$ excursions in Archean shales

The carbon isotope record also provides valuable information about the evolution of the biosphere before the GOE. Highly ^{13}C-depleted kerogens occur in ~2.7 Ga shales of Western Australia, South Africa, and Canada (Hayes 1983, 1994) and have been interpreted to reflect the presence of methanotrophic bacteria. These organisms oxidize methane, potentially utilizing a wide variety of oxidants (oxygen, nitrite, sulfate, and Mn+Fe oxides; Hayes 1983, 1994; Hinrichs 2002; Beal et al. 2009; Ettwig et al. 2010). The source of methane appears to have been methanogenesis, which is inferred to have been a common metabolic pathway in organic matter-rich and sulfidic shales associated with iron formation sequences, as well as in precursor sediments for iron formations in Archean and Paleoproterozoic oceans (e.g., Konhauser et al. 2005). In this scenario, methane produced in sediments during early diagenesis was incorporated into organic matter. Although the earliest interpretations of this process called for an oxidation gradient and suggested free oxygen, this may not be a requirement because of the possibility of oxidation by other oxidants (Beal et al. 2009).

---

[2] The delta notation (e.g., $\delta^{13}C$, $\delta^{15}N$ values) describes the permil level deviation of an isotope ratio in a sample from that in a reference material. Equations for these notations are: $\delta^{13}C = ((^{13}C/^{12}C)_{sample}/(^{13}C/^{12}C)_{reference} - 1)$ and $\delta^{15}N = ((^{15}N/^{14}N)_{sample}/(^{15}N/^{14}N)_{reference} - 1)$.

Kerogen in shales associated with the ~2.5–2.45 Ga iron formations is also ^{13}C-depleted (e.g., Beukes et al. 1990), although not as dramatically as in ~2.7 Ga lithologies. Similarly depleted carbon isotope values were observed in shales overlying Paleoproterozoic glacial deposits in North America and South Africa, and in shales deposited after and during the Lomagundi carbon isotope excursion in Karelia, Russia, and in Francevillian Basin, Gabon (Gauthier-Lafaye and Weber 1989; Melezhik et al. 1999; Coetzee 2001; Bekker and Kaufman 2007). These values were linked with methane cycling across a redoxcline developed in Paleoproterozoic basins during and in the aftermath of the rise of atmospheric oxygen. Notably, the sedimentary successions that contain the latter Paleoproterozoic shales do not include iron formations.

The nitrogen isotope record

Cyanobacterial production of oxygen on the early Earth would also have had a significant impact on the marine nitrogen cycle, and this relationship is recorded by the δ^{15}N values of marine organic matter. In the modern oxygenated oceans, the nitrogen cycle is controlled by a balance between the supply of dissolved inorganic nitrogen via biological reduction of atmospheric N_2 to NH_4^+ (by nitrogen fixation), and the loss of fixed N to the atmosphere via denitrification (conversion of NO_3^- to N_2) and anaerobic ammonia oxidation (anammox), i.e., oxidation of NH_4^+ to N_2 utilizing NO_2^- (Dalsgaard et al. 2005) (Fig. 4). Nitrate (NO_3^-) is produced by nitrification, the stepwise oxidation of ammonium to nitrite and nitrate, which requires at least some free oxygen (Carlucci and McNally 1969). Nitrite (NO_2^-) is produced both by nitrification and by nitrate reduction (e.g., Lam et al. 2009); both processes also require molecular oxygen. In Earth's early oceans before oxygenic photosynthesis, the oxidative processes would have been absent, and the nitrogen cycle would have consisted solely of N_2 fixation followed by burial and regeneration of NH_4^+ in sediments (Fig. 4). Note that anaerobic ammonium oxidation coupled with sulfate reduction has also recently been proposed as a thermodynamically feasible metabolic pathway in modern sediments (Schrum et al. 2009). This pathway remains to be demonstrated biochemically; however, if it indeed exists, or did so in the geologic past, it might have been relevant to the nitrogen cycle on the anoxic early Earth, where photochemically produced sulfate aerosols were delivered from the atmosphere to the oceans and sediments.

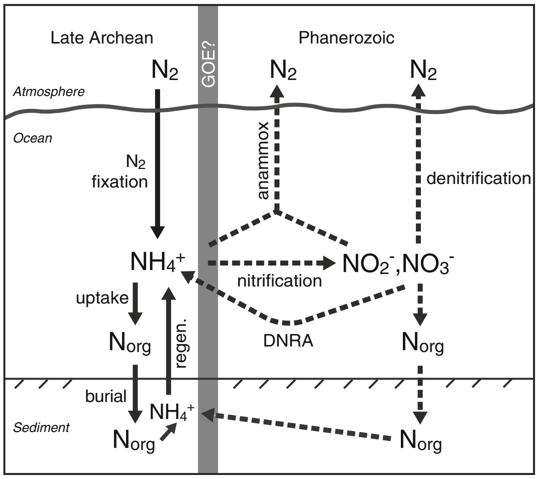

Fig. 4 Cartoon of the global N cycle, depicting the major processes that contribute to the δ^{15}N values of organic matter in the modern oceans, and presumably organic matter and NH_4^+ (structurally incorporated into clays) in ancient sediments. The *dashed arrows* depict processes that require oxidation of ammonium to produce nitrate or nitrite, and are therefore inferred to have been largely absent on an early anoxic Earth. The production of oxygen by cyanobacteria (during the GOE or possibly earlier) would have facilitated these oxidative processes, leading to a fundamental change in the global N cycle to the one depicted here for the Phanerozoic. Note that in an early Archean atmosphere, a second source of fixed N would have been the abiotic production of nitric oxide (NO) by lightening, requiring the splitting of CO_2 and H_2O (Navarro-Gonzalez et al. 2001); however, Kasting and Siefert (2001) suggested that the low concentrations of CO_2 on the early Earth could have limited the amount of NO formation, selecting for biological N_2 fixation as early as ~3.5 Ga before present

Nitrogen fixation produces organic nitrogen that is similar to or depleted in ^{15}N relative to atmospheric nitrogen (δ^{15}N values from ~0 to −3‰ with respect to atmospheric N_2; see review in Zerkle et al. 2008). Denitrification (and presumably also anammox) returns ^{15}N-depleted N_2 to the atmosphere, leaving the residual NO_3^- (and resulting organic N) relatively enriched in ^{15}N by greater than 20‰ (Wellman et al. 1968; Delwiche and Steyn 1970; Miyake and Wada 1971). In ancient anoxic oceans, N_2 fixation and uptake of isotopically light regenerated ammonium led to the burial of organic matter with primarily negative δ^{15}N values, as low as −6‰ (see compilation in Papineau et al. 2005). In modern oxygenated oceans, nitrification and denitrification processes drive sedimentary organic matter toward ^{15}N-enrichment, producing average δ^{15}N values of +6 to +7‰ (Peters et al.

1978; Sweeney et al. 1978). The increase in δ^{15}N values reflecting the introduction of oxidative pathways to the nitrogen cycle (via ocean oxygenation) forms the basis for application of nitrogen isotopes to the study of the history of oxygenic photosynthesis, surface oxygenation, and oxidation of the oceans.

Significantly ^{15}N-depleted values (down to −6‰) have only been measured in sedimentary organic matter deposited before the GOE and in black shales deposited during periods of widespread ocean anoxia in the Phanerozoic (see compilation in Papineau et al. 2005). The negative δ^{15}N values in the Phanerozoic are commonly attributed to increased N_2 fixation necessitated by removal of fixed N by denitrification and anammox in anoxic basins or in expanded oxygen-minimum zones, usually associated with enhanced phosphate release from anoxic sediments (e.g., Kuypers et al. 2004; Sachs and Repeta 1999; Junium and Arthur 2007). Since both denitrification and anammox require oxidation of ammonia with molecular oxygen, as discussed above, this type of explanation requires the previous establishment of an oxidative N cycle, and thus is probably not applicable to the Archean record beyond transient oxidation events. The shift toward more positive δ^{15}N values of organic matter at the end of the Archean instead appears to record a fundamental change in the nitrogen cycle coincident with, and likely due to, the oxygenation of the Earth's oceans.

Trends in δ^{15}N values across the GOE

Beaumont and Robert (1999) were the first to document a change in the δ^{15}N values of Archean and Proterozoic marine kerogen. They reported δ^{15}N values that were mostly negative (<-2 ‰) in Archean samples and that shifted to positive values (+2 to +10‰), typical of the modern ocean, between ~2.5 and 2.1 Ga. Sedimentary δ^{15}N values remain predominantly >0‰ throughout the rest of Earth history, except for the Phanerozoic black shales deposited during periods of widespread ocean anoxia, as discussed above. The change in the δ^{15}N values of kerogen observed by Beaumont and Robert (1999) was interpreted to reflect a change in the global N cycle associated with the development of nitrification and denitrification, resulting in a loss of isotopically light N to the atmosphere (Beaumont and Robert 1999; Papineau et al. 2005). This change was associated with the oxygenation of Earth's surface environments because of the necessity of oxygen for nitrification. An alternate hypothesis attributes negative δ^{15}N values in Archean sediments to ^{15}N-depleted mantle sources, suggesting that the change in δ^{15}N values is connected to the intensity of hydrothermal activity rather than oxidation of surface environments (Jia and Kerrich 2004; Jia 2006; Pinti and Hashizume 2001, Pinti et al. 2009). However, there remains strong evidence for a sedimentary, rather than a hydrothermal origin for at least some of the rock in question (e.g., Papineau et al. 2005).

Recent studies by Garvin et al. (2009) and Godfrey and Falkowski (2009) have documented shifts to more positive δ^{15}N values of organic matter within sedimentary successions as old as ~2.67 Ga, and thus deposited before the GOE. These δ^{15}N variations are also interpreted to reflect changes in the cycling of nitrogen related to oxygenation. The trend toward more positive δ^{15}N values is interpreted by both groups to reflect an increase in N loss due to denitrification and anammox, implying the onset of an oxidative N cycle nearly 200 million years before the oldest unequivocal geological indicators for extensive long-term surface oxygenation. These studies demonstrate trends in nitrogen isotope data from well-characterized core material that imply changes in the nitrogen cycle potentially related to oxygen. If the connection to oxygen is verified, it will be important to document just how far back these signals extend and how sensitive this proxy is to the presence of oxygen in these ancient environments. It remains unclear whether low-level atmospheric oxidation is required to produce these trends or whether they reflect an oceanic (surface ocean) oxidation event.

Sources of negative δ^{15}N values in the Archean Biosphere

The studies described above attribute a general increase in δ^{15}N values to the onset of an aerobic N cycle; however, a number of the mechanisms suggested to explain the predominance of negative δ^{15}N ratios in Archean organic matter further invoke ocean anoxia. Cyanobacteria are the primary source of fixed N to the modern oceans (e.g., Carpenter and Romans 1991). Culturing studies have demonstrated that modern N_2-fixing cyanobacteria only produce significantly negative δ^{15}N values when grown under Fe-replete conditions (Zerkle et al. 2008). If the biochemical mechanism for N_2 fixation has not changed significantly since its evolution early in Earth history (e.g., Dean and Jacobson 1992), enhanced Fe availability in the surface waters during periods of ocean anoxia (both in the Archean and in the Phanerozoic) could therefore have contributed to the production of organic matter with negative δ^{15}N values during these periods (Zerkle et al. 2008).

However, even at high Fe concentrations, N_2-fixing cyanobacteria in cultures and in modern environments have only produced organic matter with δ^{15}N values down to −3.6‰. Thus, this process alone cannot explain the much lower N isotope values, down to −6‰, reported for Archean sediments (Beaumont and Robert 1999; Pinti and Hashizume 2001; Papineau et al. 2005; Pinti et al. 2009). One model for generating ^{15}N-depleted values in anoxic systems (e.g., Fry et al. 1991; Voss et al. 1997; Coban-Yildiz et al. 2006; Junium and Arthur 2007; Papineau et al. 2009) invokes the uptake of isotopically light ammonium formed by the degradation of organic N in sediments and in the lower part of the water column.

A second explanation for the negative N isotope values measured before the GOE is that a different dominant organism supplied fixed N to the Archean biosphere. Pinti et al. (2001, 2009) suggested that the negative δ^{15}N values measured in Archean sediments could reflect N_2 fixation from ^{15}N-depleted magmatic sources by chemosynthetic hydrothermal vent communities, although many of the samples analyzed show evidence of shallow-marine sedimentary origin as discussed above. A more intriguing possibility is the contribution of anoxygenic phototrophs to the Archean N cycle. Many anoxygenic phototrophs (including purple and green sulfur bacteria) are capable of fixing nitrogen (Lindstrom et al. 1950; Wahlund and Madigan 1993). Molecular biomarkers for some anoxygenic phototrophs (isorenieratene, derived from green sulfur bacteria) have been found in sediments of several Phanerozoic euxinic basins with ^{15}N-depleted organic matter (Joachimski et al. 2001; Sinninghe Damste and Koester 1998; Pancost et al. 2004; Cao et al. 2009). The little data available suggest that these organisms produce chlorophyll that is significantly more depleted in ^{15}N than N_2-fixing cyanobacteria (Sachs et al. 1999; Beaumont et al. 2000; Ohkouchi et al. 2005). These molecules are similar to ^{15}N-depleted geoporphyrins (N-rich biomolecules believed to be derived from chlorophylls) that have been found in Phanerozoic sediments with negative δ^{15}N values, which were previously attributed to cyanobacteria and used to argue for N_2-fixing organisms as the primary contributor of organic matter to the sediments (Chicarelli et al. 1993; Sachs and Repeta 1999; Ohkouchi et al. 2006; Kashiyama et al. 2008). Molecular biomarkers from anoxygenic phototrophs have yet to be reported from Archean sediments; however, these organisms could have provided another source of organic matter with negative δ^{15}N values to the Archean biosphere. This possibility would be consistent with the other lines of evidence, supporting a greater contribution of fixed N from oxygenic phototrophs and the onset of aerobic N cycling following increased ocean oxidation during the GOE.

The sulfur isotope record

Sulfur has one of the most extensive isotope records and is strongly linked to oxygen. Assembly of the secular S isotope record has occurred in several phases and continues today. The earliest reported sulfur isotope analyses were done in the late 1940s by Thode et al. (1949), and culminated in the classic studies of Perry et al. (1971), Monster et al. (1979), Hattori et al. (1983a, b; 1986), and Cameron (1982, 1983). These studies documented a change in the range of values for ^{34}S/^{32}S ratio (δ^{34}S) from a narrow range centered on mantle values (~0‰) prior to ~2.45 Ga to a range of ~25‰ after ~2.45 Ga. This pattern is illustrated with the compilations in Fig. 5 and with the histograms in Fig. 6. More recent studies (e.g., Farquhar et al. 2000; Bekker et al. 2004; Papineau et al. 2007; Guo et al. 2009) have argued for a change in the relationships between ^{33}S/^{32}S and ^{34}S/^{32}S ratios (Δ^{33}S) and in some cases between ^{36}S/^{32}S and ^{34}S/^{32}S ratio (Δ^{36}S). Ties of these records to atmospheric oxygenation are discussed below.

Secular changes in δ^{34}S values

The long-term evolution of the sulfur isotope record has been interpreted to reflect the response of sulfate-reducing prokaryotes to changes in oceanic sulfate concentrations. At low sulfate concentrations, the uptake and reduction of sulfate by microorganisms does not result in significant discrimination between sulfur isotopes and, therefore, does not produce significant fractionations. This has been known since the pioneering study of Harrison and Thode (1958) and was later reinforced by the models of Rees (1973). It has been part of the explanation for the secular trend in the fractionation between sulfate and sulfide since the early studies of Monster et al. (1979), Hattori et al. (1983a, b, 1986), and Cameron (1982, 1983), who argued that the smaller range of fractionations measured in Archean sediments reflects low sulfate concentrations in the Archean oceans. These early arguments have been extended and strengthened by more recent studies of Canfield et al. (2000) and Habicht et al. (2002), who have reexamined the metabolic response to low sulfate concentrations. These workers further extended the connection to sulfate concentrations, using diagenetic models that coupled sulfate reduction rates and sulfate transport within non-bioturbated sediment. This aspect of their work, in combination with the calibration of the rates of sulfur metabolisms, allowed them to identify a threshold of sulfate concentrations of ~200 μM, below which the fractionations produced are within the range observed in the Archean. They inferred that Earth's early oceans had sulfate concentrations at or below this level, supporting a lack of significant oxidative weathering on a largely anoxic Earth.

Interpretation of minor sulfur isotopes

Further constraints on oceanic and atmospheric redox states can be gained from investigation of minor sulfur isotopes in addition to traditional δ^{34}S studies. Sulfur has four stable isotopes (^{32}S, ^{33}S, ^{34}S, and ^{36}S) and preserves additional information via the co-variance of the three S isotope ratios (^{33}S/^{32}S, ^{34}S/^{32}S, and ^{36}S/^{32}S). The most common way to

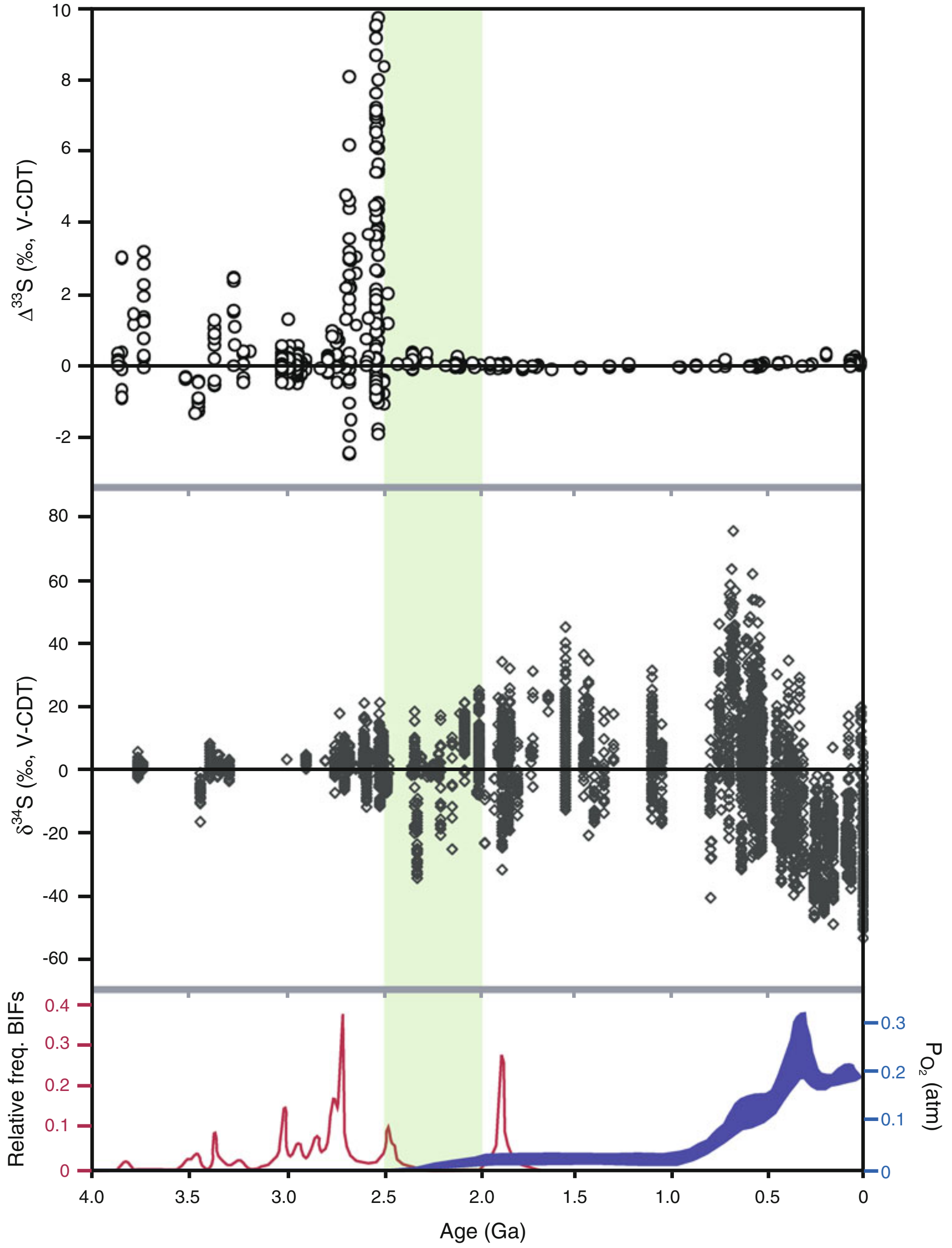

Fig. 5 Compilation of δ^{34}S values for sedimentary sulfides and sulfates (modified from Canfield and Farquhar 2009). Plot of Δ^{33}S values for sedimentary and metasedimentary rocks on the middle panel is modified from Domagal-Goldman et al. (2008). Relative frequency of BIFs is shown in *red* (Isley and Abbott 1999) and pO_2 curve in *blue* (Holland 2009) against geological time on the lowermost panel

describe these co-variations is by defining two terms, Δ^{33}S and Δ^{36}S values that describe the deviation from a reference relationship between $^{33}S/^{32}S$, $^{34}S/^{32}S$, and $^{36}S/^{32}S$ ratios.[3]

The records of Δ^{33}S and Δ^{36}S values provide evidence for a striking change in the terrestrial sulfur cycle related to the oxidation of Earth's surface environments (Fig. 5) (Farquhar et al. 2000; Kasting 2001; Pavlov and Kasting 2002; Farquhar and Wing 2003; Bekker et al. 2004; Papineau et al. 2007; Guo et al. 2009). This change from sulfur carrying a mass-independent S isotope signal, with large non-zero Δ^{33}S values and strongly correlated Δ^{36}S values, to a dominantly mass-dependent S isotope signal, with very small Δ^{33}S and Δ^{36}S values, occurred sometime between ~2.45 and 2.32 Ga.

---

[3] The delta notation (δ^{34}S) describes the permil level deviation of an isotope ratio in a sample from that in a reference material, and the capital delta notation (Δ^{33}S and Δ^{36}S) describes the deviation of an isotope ratio from a reference fractionation array. Equations for these quantities are: $\delta^{34}S = (^{34}S/^{32}S)_{sample}/(^{34}S/^{32}S)_{reference} - 1)$ and $\Delta^{33}S = (^{33}S/^{32}S)_{sample}/(^{33}S/^{32}S)_{reference} - [(^{34}S/^{32}S)_{sample}/(^{34}S/^{32}S)_{reference}]^{0.515}$ and $\Delta^{36}S = (^{36}S/^{32}S)_{sample}/(^{36}S/^{32}S)_{reference} - [(^{34}S/^{32}S)_{sample}/(^{34}S/^{32}S)_{reference}]^{1.9}$, and the values are given in permil.

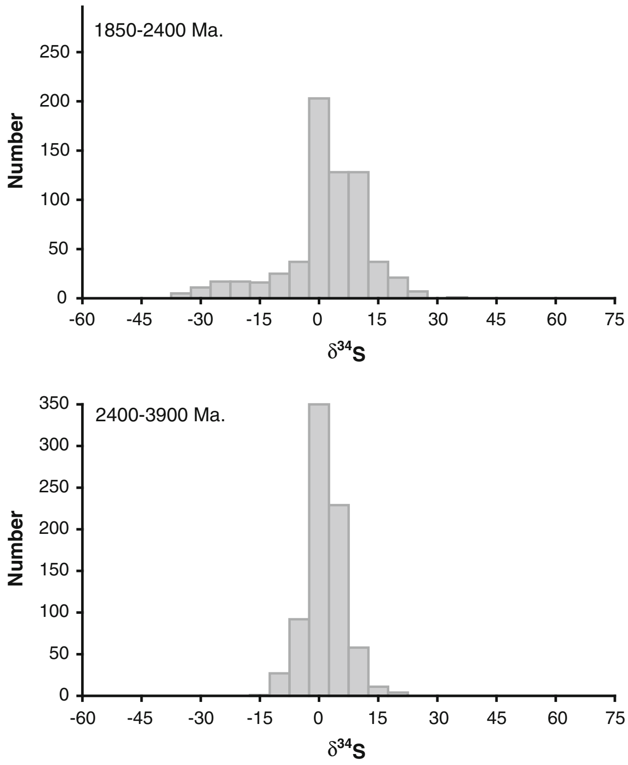

Fig. 6 Histograms of δ^{34}S values from Fig. 5. Height of *y*-axis is determined by the total number of data in interval

Arguments that link the Δ^{33}S and Δ^{36}S records to atmospheric oxygen have been made in a number of different ways. Farquhar et al. (2000) argued that the relationship between Δ^{33}S and Δ^{36}S values indicates that the signal originated from an atmospheric reaction.[4] They further suggested that the preservation of the signal in the rock record indicates that oxidative weathering to produce sulfate and microbial reduction of dissolved sulfate in the oceans were less intense prior to 2.45 Ga than today. These arguments were extended by the atmospheric models of Kasting (2001) and Pavlov and Kasting (2002), who used a different approach that relies on a calibration of the pathways for the transfer of the sulfur isotopic signal from the atmosphere to the surface (Kasting 2001; Pavlov and Kasting 2002) (Fig. 7 modified from Kasting 2001).

Farquhar et al. (2000) inferred that the disappearance of a mass-independent signal in sulfur isotopes "might represent the onset of a process capable of homogenizing mass-independently fractionated sulfur reservoirs or the suppression of one or more atmospheric reactions that had occurred before this interval." One suggestion was that the atmospheric source reactions were suppressed by changes in the abundance of absorbing species, specifically of stratospheric ozone, with ozone abundance linked to the presence or the absence of atmospheric oxygen. This link to oxygen and the coherent stratigraphic trends of δ^{34}S, Δ^{33}S, and Δ^{36}S values on different continents have made minor sulfur isotopes one of the strongest arguments for a significant change in atmospheric oxygen and form the basis for pinpointing the timing of the GOE as discussed in more detail below. By ~2.32 Ga, this early mode of sulfur cycling, with widespread transfer of a mass-independent sulfur isotope signal to the rock record, had been replaced by a sulfur cycle with higher seawater sulfate content and larger mass-dependent sulfur isotope fractionations (Fig. 8). There is no evidence of mass-independent sulfur isotope effects in the rock record since that time.

The transition between a "smaller-scale" mass-independent sulfur cycle to a "larger-scale" mass-dependent sulfur cycle with more significant oxidative weathering, higher sulfate content in the oceans, and the expression of sulfur isotope signals associated with microbial sulfate reduction was explored by Guo et al. (2009). On plots of Δ^{33}S versus δ^{34}S and Δ^{36}S versus Δ^{33}S this transition is represented by the isotopic signal evolving along a curved trajectory where a mass-independent signal largely disappears before large mass-dependent fractionations appear in the record (Fig. 8). This transition should postdate the appearance of oxygen as a stable and abundant atmospheric component on a timescale that reflects the residence time of sulfate in the ocean at that time.[5] The form of this trajectory was found to depend on the way that a growing contribution of mass-dependent sulfate derived by oxidative continental weathering was admixed to the oceanic pool (dilution of the mass-independent signal) and also on the metabolic response of sulfate reducers to rising sulfate concentrations (ingrowth of a large range for mass-dependent fractionations). While a clear progression from large to small mass-independent signals is not captured, the general form of the transition is seen by Guo et al. (2009) in the Duitschland Formation, South Africa, and this succession has been interpreted to capture the GOE. The transition in the Duitschland Formation is interrupted by a depositional hiatus (Bekker et al. 2001) and this may be

---

[4] See appendix for additional discussion of experimental evidence used to assign an atmospheric origin.

[5] Guo et al. (2009) developed a first-order kinetic model assuming that the sulfate sink is proportional to the seawater sulfate concentration. The model relies on a residence time that was derived from the present-day ~12 million year residence time of sulfate in the oceans. Their treatment therefore yielded a relaxation time for the transition equivalent to several times the modern seawater sulfate residence time. However, the residence time of sulfate in the oceanic pool most likely does not follow first-order kinetics over the range of seawater sulfate concentrations inferred for geologic time. It was most likely shorter during the GOE, and therefore the transition also would have been shorter than modeled by Guo et al. (2009). Nevertheless, the progression from mass-independent to mass-dependent relationships would have been similar.

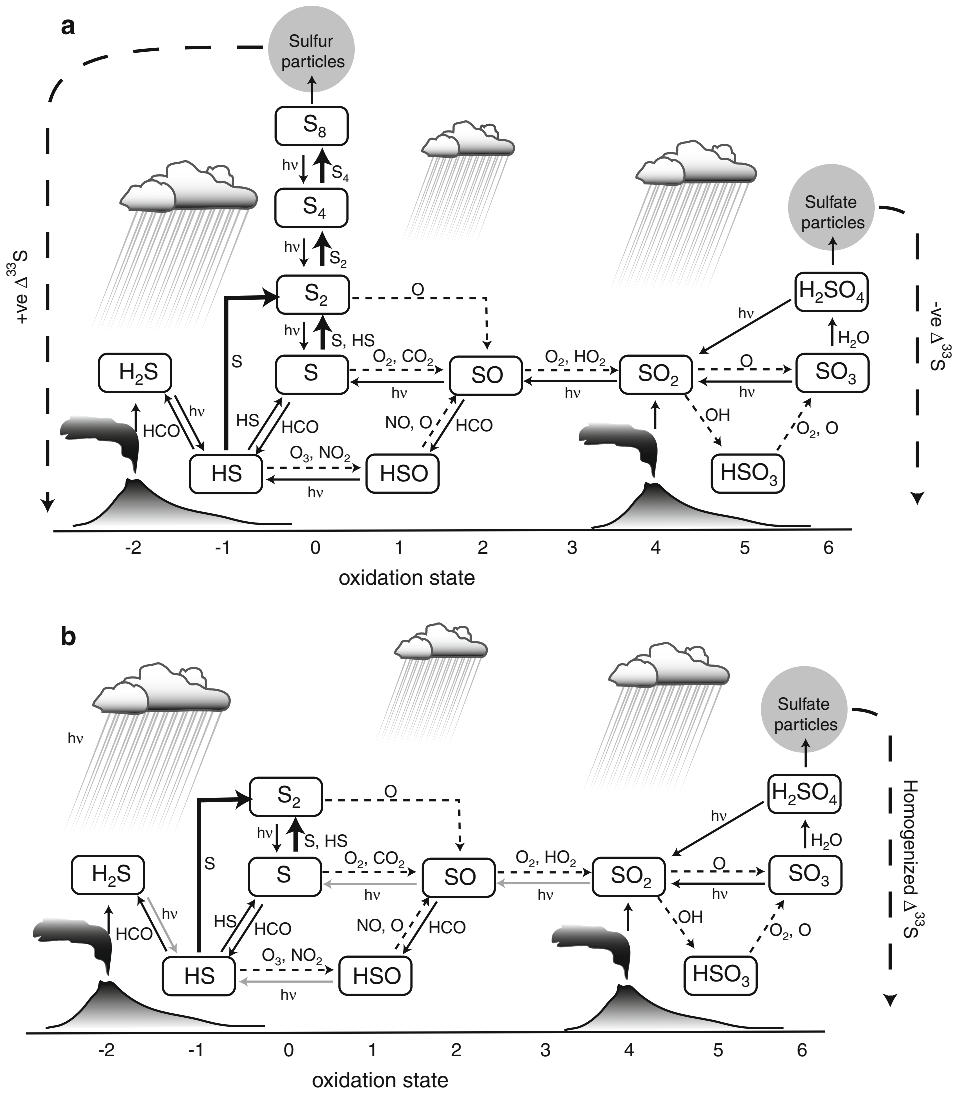
a
Sulfur particles
S_8
hν
S_4
S_4
hν
S_2
S_2
O
hν
S, HS
S
H_2S
S
O_2, CO_2
SO
O_2, HO_2
SO_2
O
SO_3
hν
hν
hν
hν
HCO
HS
HCO
NO, O
HCO
OH
O_2, O
O_3, NO_2
HS
HSO
hν
HSO_3
Sulfate particles
H_2SO_4
hν
H_2O
+ve $\Delta^{33}S$
-ve $\Delta^{33}S$
-2
-1
0
1
2
3
4
5
6
oxidation state
b
hν
Sulfate particles
S_2
O
H_2SO_4
hν
hν
S, HS
H_2O
S
S
O_2, CO_2
SO
O_2, HO_2
SO_2
O
SO_3
H_2S
hν
hν
hν
hν
HCO
HS
HCO
NO, O
HCO
OH
O_2, O
O_3, NO_2
HS
HSO
hν
HSO_3
Homogenized $\Delta^{33}S$
-2
-1
0
1
2
3
4
5
6
oxidation state

Fig. 7 Modified from Kasting (2001) and Pavlov and Kasting (2002), pathways for the physical deposition of sulfur-bearing aerosols in an anoxic world (**a**) and an oxic world (**b**). Changes in the pathways impact the efficiency with which an atmospheric isotope signature is transferred to the surface and preserved in sediments. The control is tied to oxygen levels [oxidation reactions and availability of UV—*dashed arrows* in (**a**, **b**), and *gray arrows* in (**b**), respectively]. In a low oxygen atmosphere, there are two principal pathways for the removal of sulfur-bearing aerosols. The reaction rates associated with the oxidation of S, S_2, SO, and SO_2 depend on the concentration of oxygen-bearing species, but once these species are oxidized to sulfate, it is delivered with aerosols to the Earth's surface. When the sink for species, like S_2, is insufficient to consume it completely, this species accumulates and reacts by self-reaction to form higher order sulfur species, ultimately sulfur aerosols. This opens a second pathway for physical transfer of the sulfur to Earth's surface, and ultimately to the rock record. The threshold for the opening of this pathway was constrained to be approximately 10^{-5} PAL (10^{-6} bar) (Pavlov and Kasting 2002), but is sensitive to the concentration of atmospheric sulfur (Ono et al. 2003)

part of the reason why the details of the progression are not reproduced.

The available data favor a strong connection between the presence of a mass-independent sulfur isotope signal in the rock record and low levels of free oxygen in the atmosphere and oceans. The replacement of a mass-independent signal by a mass-dependent sulfur signal (e.g., Guo et al. 2009) points to a significant accumulation of oxygen before ~2.32 Ga. This provides a minimum age constraint for the GOE and also for the time when oxygenic photosynthesis became well established, was widely distributed on Earth, and recognizably affected biogeochemical cycles.

Other stable isotope records of oxygenation

A number of other stable isotope records have been assembled or are currently being assembled that point to changes across the interval straddling the Late Archean and Early

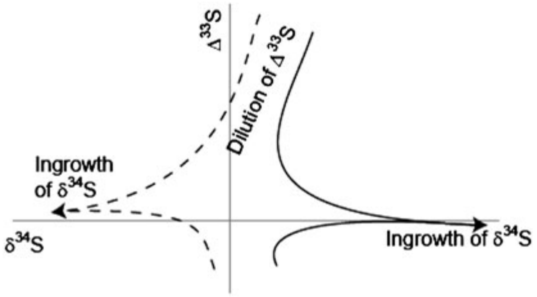
Δ^{33}S
Dilution of Δ^{33}S
Ingrowth of δ^{34}S
δ^{34}S
Ingrowth of δ^{34}S

Fig. 8 Cartoon illustrating how sulfide (*dashed lines*) and sulfate (*solid black lines*) with positive and negative Δ^{33}S values evolve in a model system where an influx of sulfate to the oceanic pool causes dilution of sulfur and ingrowth of a large sulfur reservoir exhibiting mass-dependent sulfur isotope fractionations (modified from Guo et al. 2009)

Paleoproterozoic, including those of transition metals (e.g., δ^{56}Fe, δ^{98}Mo, and δ^{53}Cr values). Transition metal stable isotopes have only recently received attention due to significant analytical advances in mass spectrometry (e.g., Arnold et al. 2004a). These isotope systems provide more information about biogeochemical cycling and redox-controlled global budgets than concentration data alone, which are discussed above for Fe and Mo. These isotope records have links to oxygenation that are complex, such as via weathering fluxes, ocean composition, and redox-dependence of oceanic sinks (e.g., δ^{98}Mo values; Arnold et al. 2004b), or that are not entirely clear (e.g., δ^{53}Cr values; Frei et al. 2009).

In particular, the sedimentary Fe isotope record has been suggested to reflect the progressive oxygenation of Earth surface environments (Rouxel et al. 2005) and even linked directly to the evolution of oxygenic photosynthesis (Johnson et al. 2008). Iron isotopes (typically reported as $\delta^{56/54}$Fe values) can be fractionated by both abiotic and biological processes, and natural variations in δ^{56}Fe values span a range of ~5‰ (see reviews in Anbar and Rouxel 2007; Johnson et al. 2008). At low temperature under equilibrium conditions, the largest Fe isotope fractionations are driven by redox transformations. Oxidized forms of Fe, both aqueous Fe^{3+} and Fe^{3+} incorporated in minerals, generally have higher δ^{56}Fe values than reduced Fe^{2+} species. Sedimentary δ^{56}Fe values exhibit a marked change at around 2.3–2.5 Ga in both pyrites and BIFs (Rouxel et al. 2005; Yamaguchi et al. 2005; Johnson et al. 2008). This change is generally interpreted to have occurred as a result of ocean oxygenation (Rouxel et al. 2005), although, the source of the isotopic signal and the dominant mechanism for fractionation is still debated (Yamaguchi and Ohmoto 2006).

Rouxel et al. (2005) argued that Fe isotope variations in sedimentary pyrites are primarily sensitive to the nature and magnitude of the oceanic removal terms and consequently the concentration of dissolved Fe^{2+} in the oceanic reservoir. They suggested that the change from a wide range of predominantly negative δ^{56}Fe values to a small range of predominantly positive δ^{56}Fe values in sedimentary pyrites at around 2.3 Ga reflects a change in the dominant removal process for dissolved Fe, from partial removal as oxides to near-quantitative removal as sulfides. These researchers hypothesized that episodic upwelling of deep-water Fe^{2+} and partial removal into BIFs via oxidation in the deep Archean ocean produced a wide range in dominantly negative δ^{56}Fe values in the residual Fe^{2+} pool that is captured in the shallow-water sedimentary pyrites. They suggested that deposition of iron formations after ~2.1 Ga was confined largely to the restricted, anoxic, hydrothermally dominated basins, and quantitative removal of Fe in an increasingly oxygenated ocean caused minimum isotope fractionation as these later stage iron formations were formed (see also Planavsky et al. 2009). At the same time, these researchers claimed that enhanced sulfate delivery via oxidative weathering led to significant removal of Fe^{2+} by pyrite formation, driving δ^{56}Fe values in pyrite more positive. Note that in order for the fractionation during pyrite formation to be expressed, this hypothesis requires that oceanic sulfate concentrations from ~2.3 to ~1.8 Ga were still sufficiently low so that all sulfide produced by sulfate reduction was titrated by dissolved Fe. Although this proposed model does not rule out biological intervention to explain the observed Fe isotope variations, it does not hold biological evolution responsible for secular changes in iron isotope composition of sedimentary minerals.

Other researchers instead interpret the Late Archean–Early Paleoproterozoic δ^{56}Fe values as reflecting processes occurring during sediment diagenesis (Yamaguchi et al. 2005; Johnson et al. 2008). They argue that the δ^{56}Fe signal in diagenetic fluids is primarily controlled by dissimilatory reduction of Fe^{3+} by microorganisms, which produces negative δ^{56}Fe values. These researchers point out that the ~3.8–3.7 Ga BIFs have a small range of positive δ^{56}Fe values similar to ~2.1–1.8 Ga BIFs, and argue that negative δ^{56}Fe values in siderites from ~2.7–2.5 Ga BIFs were due to an increase in Fe oxidation, as a direct consequence of the evolution of oxygenic photosynthesis (Johnson et al. 2008). They also link the preservation of negative δ^{56}Fe values in pyrites in Paleoproterozoic shales to an increased oxidative weathering flux of sulfate, by coupling dissimilatory iron reduction to sulfate reduction in sediments (Johnson et al. 2008). This biological model for the early Earth Fe cycle is further supported by negative C isotope values in siderites of the same BIFs (Czaja et al. 2010).

Timing and structure of the GOE

The records we have described here document a number of different types of changes resulting from the oxidation of the atmosphere and oceans during the GOE and in the period that followed. It is relevant to recognize that different geochemical proxies respond to different thresholds associated with oxidation of surface environments, and have different timescales for response.

Atmospheric oxygen, for example, is rapidly recycled by photosynthesis and respiration, but the lifetime of oxygen in the atmosphere and oceans is longer (~2 m.y.) reflecting cycling between the biosphere, sedimentary rocks (through oxidative weathering and carbon burial), and deeper Earth (via subduction of buried carbon and degassing) (Holland 2002; Catling and Claire 2005). The change in oxygen levels at the time of the GOE would have been controlled by similar processes, and the records of atmospheric and ocean oxygen levels, such as for instance sulfur isotopes, have been described above and in Fig. 5. For the present purpose, we will link the GOE to the time when the balance tipped in favor of widespread global oxygen, and we constrain this with the sulfur isotope record.

The way that oxygen rose at the time of the GOE has been traditionally viewed as a geologically rapid, stepwise transition between a state with very low levels of oxygen to a state with much higher oxygen levels, and likely involved nonlinear feedbacks involving photosynthesis and UV shielding brought about by accumulation of ozone (Kasting 1993; Claire et al. 2006; Goldblatt et al. 2006). A stable state with low oxygen levels implies a balance between oxygen sources and sinks of oxygen without a significant oxidative weathering sink. The rise of oxygen implies a time when the sources of oxygen exceeded the sinks, either as a result of a strengthening of the sources or a weakening of the sinks. In this situation, oxygen levels rose until a new sink reaction, inferred to be oxidative weathering, which is directly scaled to oxygen levels, became sufficient to balance the oxygen sources. Geochemical data that supports the view of a geologically rapid transition between states rather than a more gradual rise of oxygen has only recently become available and is preserved by the record of the Duitschland Formation in South Africa. This formation shows a transition from a small range of δ^{34}S values centered on 0 ± 10‰ V-CDT, with a clear mass-independent signal, to a larger range of δ^{34}S values, including highly positive δ^{34}S values of sulfides and carbonate-associated sulfate, without a mass-independent signal. The record of sulfur isotopes reported by Guo et al. (2009) shows that the changes in Δ^{33}S values slightly preceded the changes in δ^{34}S composition. The records are tightly coupled, however, suggesting that the disappearance of MIF was associated with a rise in seawater sulfate that became sufficient to allow for larger sulfur isotope fractionations and, therefore, highly positive δ^{34}S values of sulfides and carbonate-associated sulfate. This record also shows that the rise in δ^{34}S values is closely correlated with a rise in the δ^{13}C values of carbonates, probably reflecting enhanced oxygen production and organic carbon burial during the oldest large positive carbon isotope excursion in Earth's history (Fig. 3) (e.g., Bekker et al. 2001).

The oxygenated paleosols both below the Lorrain Formation of the Huronian Supergroup, Ontario (Ville Marie paleosols in Canada) and on the Hekpoort basalt in South Africa (Holland 1984; Prasad and Roscoe 1996; Rye and Holland 1998), sulfate evaporites in the Lucknow Formation (Schröder et al. 2008), red beds, copper stratiform deposits (Kirkham and Roscoe 1993), granular hematitic shallow-water marine ironstones, and U-enrichment in black shales appear for the first time following the GOE at 2.45–2.32 Ga (Bekker et al. 2004; Rainbird et al. 1990; Panahi et al. 2000; Partin et al. 2010). The emerging pattern from these records is that of a stepwise increase in the oxidation of surface environments which is bracketed by and closely associated with Paleoproterozoic glacial events (cf. Bekker et al. 2005; Bekker and Kaufman 2007; see Fig. 3).

A similar, high-resolution record of change has not yet been established for Mo, Re, and any other transition element for this interval, but we anticipate that these records will become available in the near future. The records that are available for these geochemical proxies point to a rapid response for U, but to a longer-term response for Mo (Scott et al. 2008; Partin et al. 2010), which may imply difference in the sensitivity of these redox-sensitive elements to oxygen, or possibly more complex responses in the Earth System. It has been suggested that some of these less studied transition element signals may track longer-term changes in atmospheric oxygen levels that followed the GOE (Rouxel et al. 2005; Frei et al. 2009).

The amount of oxygen that was produced when the balance tipped in favor of oxygen accumulation at the time of, and following, the GOE is uncertain. The present burden of freely available oxygen in today's atmosphere and oceans is on the order of 3.8×10^{19} mol (see Catling et al. 2001; Sleep and Bird 2008, and references therein). At the time of the GOE, oxygen levels are thought to have been a few percent of present levels (Yang and Holland 2003). Today, the oxygen balance is completed by considering buried carbon and sulfide as well as "excess" oxygen that has accumulated in minerals and ions in the crust and oceans as well as oxygen associated with ferric iron (Fe^{3+}) in subducted oceanic crust (Lecuyer and Ricard 1999; Sleep and Bird 2008). Sinks such as those related to oxidative weathering (estimated to be equivalent to $15.8\ (\pm 6.7) \times 10^{12}$ mol O_2/year; Holland 2002) would have played a part in the aftermath of the GOE and need to be taken into account in estimates of oxygen burden at this time.

Evidence for low-level oxygenation before the GOE

The evidence presented above converges on an interpretation of pervasive oxidation of early Earth environments initiated sometime after 2.45 Ga and reaching a fully oxygenated atmosphere by 2.32 Ga.[6] This is taken to indicate a time when cyanobacteria and oxygenic photosynthesis were well established. Other lines of evidence, including microfossils and molecular biomarkers, appear to point to a more ancient origin for cyanobacteria and thus for oxygenic photosynthesis (e.g., Sessions et al. 2009 and accompanying papers in this volume. However, for a different view see Kopp et al. 2005; Kirschvink and Kopp 2008; Rasmussen et al. 2008). A large body of evidence bearing on transient oxygenations earlier in Earth's history has additionally been collected in recent studies of drill cores through Late Archean successions in Western Australia and South Africa (Anbar et al. 2007; Kaufman et al. 2007; Garvin et al. 2009; Godfrey and Falkowski 2009; Kendall et al. 2010). We will briefly examine some of this evidence and evaluate the arguments below.

Studies of the ABDP-9 core drilled in Western Australia through the ~2.50 Ga Mount McRae Shale (Anbar et al. 2007) have documented several lines of geochemical evidence pointing to a change in the chemical nature of the Earth's oceans and atmosphere during deposition of the upper part of this formation (Fig. 9). Kaufman et al. (2007) documented a change in the relationship between the four stable isotopes of sulfur at ~153-m depth in the Mount McRae Shale core. Sediments in the lower part of the section are characterized by positive Δ^{33}S values that are positively correlated with δ^{34}S values, while sediments in the upper part are also characterized by positive Δ^{33}S but predominantly negative δ^{34}S values (Kaufman et al. 2007; Fig. 9).

The positive correlation between δ^{34}S and Δ^{33}S values in the lower part of the Mount McRae Shale is interpreted to reflect either a primary atmospheric signal, or mixing among atmospheric, terrestrial, and juvenile sources (Ono et al. 2003; Kaufman et al. 2007). These two hypotheses are difficult to distinguish, because they may share some of the same end-members for sulfur sources, but both call for a role of atmospheric chemistry. A similar relationship was observed for δ^{34}S and Δ^{33}S values of sulfides from correlative successions in the South African AD-5 core by the same authors.

One interpretation of the negative δ^{34}S values of sulfides in the upper part of the unit is that they reflect a shift of the location of sulfate reduction from the sediments into the water column and, possibly, the establishment of an oxidative part in the sulfur cycle (Kaufman et al. 2007). It has also been suggested that sulfate concentrations may have risen at this time (Kaufman et al. 2007; Reinhard et al. 2009) via oxidative continental weathering. It is not clear if this latter assertion can be reconciled with the mass-balance constraints imposed by the mass-independent signal throughout the succession. The persistence of this signal sets the upper limit on atmospheric oxygen, and also implies that sulfate flux from the continents (and juvenile hydrothermal sources) could not have been significantly larger than volcanic sulfur flux. It has also been suggested that the different slopes of Δ^{36}S/Δ^{33}S in the lower and upper parts of the Mount McRae Shale and the time-equivalent Gamohaan Formation of South Africa imply a change in atmospheric chemistry (Kaufman et al. 2007). Alternatively, this change may reflect an overprint of sulfate reduction on atmospherically-derived sulfate, as was interpreted for the older successions by Shen et al. (2009) and Ueno et al. (2009).

Trends in the concentrations of transition elements (Mo and Re; Anbar et al. 2007; Kendall et al. 2010), iron speciation (Reinhard et al. 2009; Poulton et al. 2009; Kendall et al. 2010), and Cr isotopes (Frei et al. 2009) have been interpreted to indicate low-level transient oxidation during the same period. Anbar et al. (2007) documented an enrichment in authigenic Mo and an increase in the Mo/TOC ratios of euxinic shales from between 153- and 143-m depth in the Mt. McRae Shale core (Fig. 9), indicating that small amounts (<1% of the Mo inventory in the modern ocean; Anbar et al. 2007) of dissolved Mo were present at the depositional site. This is interpreted to reflect Mo delivery by oxidative weathering, but at much lower levels than at present. These researchers cite a correlative enrichment in Re as supporting evidence for low levels of oxidative weathering, since Re has a similar chemistry to Mo. The shales lack a U enrichment, but this is argued to reflect oxidative weathering of sulfides, while uranium is predominantly hosted in silicates, which are indifferent to atmospheric oxygen level. Mo and Re enrichments are not present lower in the core (from ~170- to 190-m depth), and decrease above ca. 143 m, indicating a drop in the dissolved Mo seawater inventory (Anbar et al. 2007).[7] Finally, studies of nitrogen isotopes of the Mount McRae Shale from the ABDP-9 core documented a change from values of ~+2.5‰ below 161-m depth up to +7.5‰ between 161- and 139-m depth, and back down to ~+2.5‰ above 139-m depth (Fig. 9), potentially reflecting contribution from nitrification and denitrification associated with the temporary onset of an aerobic nitrogen cycle (Garvin et al. 2009).

---

[6] Oxygenation likely continued during the Lomagundi carbon isotope excursion but we are concerned here about the first pervasive oxidation reflected by the transition from MIF to MDF of sulfur isotopes.

[7] We add the cautionary note that the role of hydrothermal activity which has clearly affected other records (e.g., Isley 1995; Barley et al. 1997, 1998; Isley and Abott 1999; Condie et al. 2001) is unclear and should be carefully considered in directly tying this evidence to low level transient oxygenation and oxidative weathering of sulfide minerals. As discussed above, low-temperature hydrothermal Mo flux could have been quantitatively important under Archean anoxic conditions.

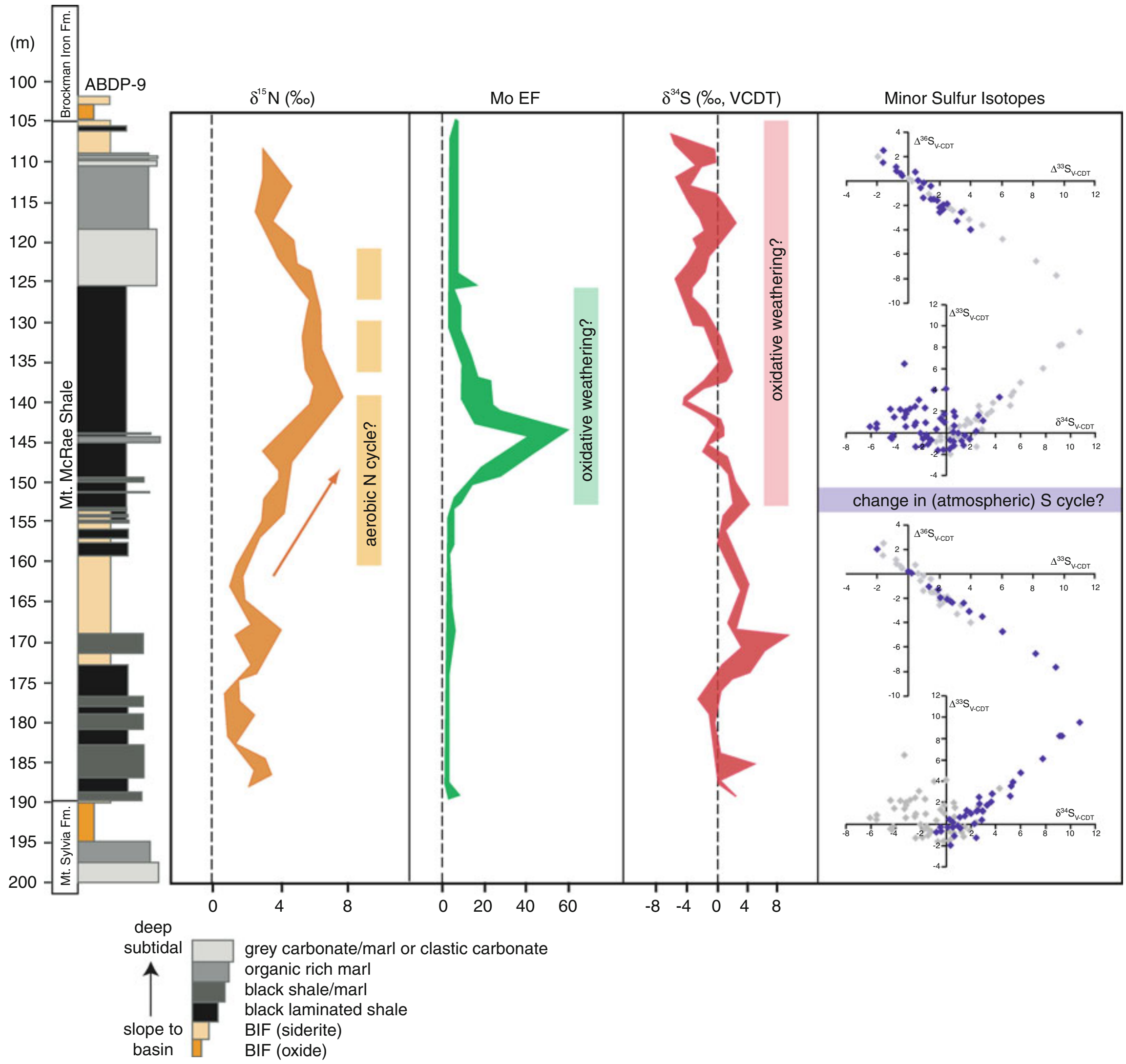

Fig. 9 Compilation of geochemical trends [Mo enrichment factors (Mo EF) from Anbar et al. (2007), S isotopes from Kaufman et al. (2007), and δ^{15}N values from Garvin et al. (2009)] and the associated interpretations used to argue for the occurrence of transient oxygenation during deposition of the ~2.5 Ga Mount McRae Shale, Western Australia (see text for detailed discussion). Sulfur isotope data are divided into *upper* and *lower* intervals. Data outside the stratigraphic interval is shown in *light grey*, while data from the stratigraphic interval are in *blue*

Studies of other drill cores from South Africa, including the AD-5 and GKP01 cores, suggest less pronounced Mo and Re enrichments above the crustal levels and similar sulfur and nitrogen isotope patterns in contemporaneous and even older successions. A study by Wille et al. (2007) and Kendall et al. (2010) examined several drill cores from South Africa, including the GKP-01 drill core through the ~2.64–2.48 Ga Ghaap Group, and samples from older successions. They also observed a secular change in the Mo and Re concentrations and Mo isotope compositions starting before and extending through the ~2.64–2.48 Ga time interval. These workers also related their observations to a low-level oxygenation, but based on the age of the studied units where these observations were made, argued for an even earlier appearance of oxygen. A nitrogen isotope study of sedimentary units in the GKP01 core by Godfrey and Falkowski (2009) also shows a small increase in δ^{15}N values of organic matter, and are interpreted as indicative of aerobic N cycling from as early as 2.67 Ga. Studies of sulfur isotopes also show changes in the relationship between δ^{34}S, Δ^{33}S, and Δ^{36}S across these sedimentary units (Ono et al. 2009a, b; Kaufman et al. 2007). This has been interpreted to reflect changes in the cycling of sulfur, possibly with water column oxidation of sulfide, but without a loss of mass-independent signals. This would suggest that if there was atmospheric oxidation, it was at a very low level.

The occurrence of low-level oxygenation before the GOE implies an earlier origin for oxygenic photosynthesis, and raises questions about how production of oxygen might have been ongoing without oxygenation of the oceans and atmosphere. A number of workers have examined this question, and some (e.g., Kopp et al. 2005; Kirschvink and Kopp 2008) have argued that this condition is unlikely, and that the rise of oxygen coincided with the evolution of oxygenic photosynthesis. Others (Kasting 1993; Catling et al. 2001; Holland 2002, 2009) have argued that while oxygenic photosynthesis was a precondition for the rise of atmospheric oxygen, the operation of photosynthesis alone is insufficient for pervasive oxygenation. They call on additional factors such as organic carbon burial, hydrogen loss, and evolution in composition and fluxes of volcanic emanations to play a critical role in tipping the balance in favor of an oxidized atmosphere. These studies frame the question of Earth's surface oxidation in terms of sustainable, long-term balance between supplies of oxidants, including oxygen, and reductants that provide the sink for oxidants. Arguments have been made that any change in atmospheric oxygen level either up or down reflects a condition when the supply and sinks for oxygen are not balanced (e.g., $\frac{d[O_2]}{dt} = F_{\mathrm{Atmospheric\,H_2\_loss}} + F_{\mathrm{C\&S\_burial}} - F_{\mathrm{volcanic\&metamorphic\,gases}} - F_{\mathrm{oxidative\,weathering(Fe,C,S,...)}} \neq 0$, where F refers to the fluxes associated with oxygen production and consumption).

Various suggestions have been made to describe how the long-term sinks and sources for oxygen may have changed. These include early suggestions that call for (1) changes in mantle redox conditions (e.g., Holland 2002; Kump et al. 2000) and for (2) changes in the relative burial ratio of organic carbon (c.f., Kasting 1993; Karhu and Holland 1996), but evidence for these types of changes is inconclusive. Other suggestions have been made that call for oxidation of the surface environments as a result of (3) long-term escape of hydrogen to space (Kasting 1993; Catling et al. 2001; Catling and Claire 2005; Holland 2002; but we note that hydrogen escape rate and the factors that control it are the subject of ongoing research; Tian et al. 2005, 2008; Catling 2006; Kulikov et al. 2007) which would ultimately oxidize the Earth's surface environments, crust, and mantle. Evidence for the change in the oxidation state of the mantle that is thought to exert the principal control over the oxidation state of volcanic gases is, however, lacking (Delano 2001; Canil 2002; Li and Lee 2004). This has prompted several other suggestions, including (4) that the response of Earth's surface environments to oxygen production may have been nonlinear, and that more than one stable state may have existed under the same levels of photosynthetic oxygen production (e.g., Zahnle et al. 2006; Goldblatt et al. 2006), (5) that changes in the oxidation state of volcanic gases were associated with increasing intensity of subaerial volcanism (Kump and Barley 2007), and (6) a recent suggestion by Holland (2009) that the increasing CO_2/H_2O and SO_2/H_2O ratios of volcanic gases would evolve as a consequence of different pathways for degassing and recycling of mantle and crustal pools, *and* that this would change the reductive capacity of these gases, weakening the oxygen sinks and eventually reaching a crossover point where oxygen would accumulate. These possibilities are not necessarily mutually exclusive. A consensus has yet to be reached, but it appears that a number of possibilities exist to explain why there is a delay between oxygen production and the rise of atmospheric oxygen.

Considerations

While a growing body of evidence from a variety of geochemical sources (trace element concentration data, iron speciation data, and stable nitrogen, carbon, sulfur, and molybdenum isotope data) points to changes linked to transient oxygenation events prior to the GOE, the interpretation that there was low-level oxygenation is not irrefutable and questions remain. These relate to: (1) the timing and duration of the oxidation events as recorded by the various geochemical proxies, which does not seem to be synchronous; (2) whether the various types of evidence require only accumulation of oxygen in seawater or accumulation of oxygen at very low levels in the atmosphere; and (3) many of these proxies are newly developed, and alternative interpretations of the causes and significance of the isotopic signals may yet be developed. None of these questions provide direct evidence to refute the inferences about early oxygen production, but they do highlight areas for further investigation.

Evolution of oxygen in the aftermath of the GOE

The evolution of oxygen in the aftermath of the GOE can be used to illustrate further how oxygen levels may be partly independent of the rates of cycling by oxygenic photosynthesis and respiration. The aftermath of the GOE did not see a rise in oxygen to present levels, but instead saw a smaller accumulation of oxygen, a few percent of present levels (Holland 1984; Rye and Holland 1998; Pavlov et al. 2001). It is debated whether oxygen concentrations stabilized at these levels until a second oxidation event at the end of the Proterozoic, returned to lower levels at any time after the GOE (Bekker et al. 2006; Schröder et al. 2008; Frei et al. 2009), or rose gradually during the intervening interval between these two oxidation events (Frank et al. 2003; Kah et al. 2004; Johnston et al. 2005). It is clear that some changes occurred along with the disappearance of Superior-type iron formations between 1.8 and 1.9 Ga that most likely had some impact on Earth's surface oxidation, but the details of this change are debated (Holland 1984; Canfield 1998; Poulton et al. 2004; Slack et al. 2007; Slack and

Cannon 2009) and the absolute magnitude of the change in oxygen level is unclear. The second major rise in oxygen occurred at the end of the Proterozoic and is associated with the radiation of complex life in the oceans (Logan et al. 1995; Kaufman and Knoll 1995; Canfield and Teske 1996; Canfield et al. 2007). This second oxidation event, which is considered as important as the GOE, appears to suggest that changes in the oxygen cycle may occur independently of changes in intensity of photosynthesis and respiration, illustrating how long-term variations in oxygen levels reflect longer-term changes in oxygen sources and sinks. Suggested causes of this later oxidation event include: (1) changes in the burial efficiency of carbon associated with sinking of larger organisms that have greater biological ballast (Logan et al. 1995; Holland 2005), (2) a long-term accumulation of oxygen associated with net loss of sulfide by subduction to the mantle during the Proterozoic (Catling et al. 2002; Canfield 2004), and (3) changes in surface oxidation state related to continued hydrogen loss during the Proterozoic (Catling and Claire 2005).

Conclusions

The majority of evidence supports a self-consistent interpretation of the geologic, isotopic, and transition element data that is linked to the irreversible rise of atmospheric oxygen during the Great Oxidation Event shortly before 2.32 Ga. This age provides a solid younger bound on the origin of oxygenic photosynthesis. Some types of geochemical evidence appear to suggest low-level oxygenation in oceanic settings during the 200–300 million year interval that preceded this period, perhaps extending to the Mesoarchean–Neoarchean boundary. While the reason/s for the time lag between the onset of photosynthesis and the rise of atmospheric oxygen is/are unclear, a number of plausible working hypotheses exist that can account for this change. If it is the case that photosynthesis arose significantly before the rise of atmospheric oxygen, the trigger for oxygenation lies with the balance of sources and sinks for oxygen, and demonstrates that the oxygen cycle has more than one stable state, with a nonlinear response relating to transitions among these states. We close with one important caution. While the presence of oxygen at ~2.6–2.5 Ga would imply an earlier age for the origin of oxygenic photosynthesis, the evidence for low-level atmospheric oxidation in this interval is less robust, and considerably more work is needed to demonstrate irrefutably that this is the case. We presently do not consider that geologic evidence assembled from rocks older than the Neoarchean/Mesoarchean boundary (~2.8 Ga) provides any conclusive support for the presence of free oxygen in the Earth's surface environments.

Acknowledgments The authors thank H. D. Holland, P. Falkowski, D. Catling, C. Reinhard, and an anonymous reviewer for constructive comments on the manuscript. The discussion of transition metal stable isotopes greatly benefited from comments and editing by S. Severmann. A. Bekker acknowledges support from an NSERC Discovery Grant. J. Farquhar acknowledges support from a NASA EXB grant and the NAI.

Appendix

Experimental studies of MIF and the connection to atmospheric chemical reactions

The connection between $\Delta^{33}S$ and $\Delta^{36}S$ values and atmospheric chemistry was explored using three different approaches. The first of these was a study by Farquhar et al. (2001), who presented results of a series of closed-cell photolysis experiments with sulfur dioxide that were undertaken with a variety of light sources. These experiments produced reaction products with large isotope variations for $^{33}S/^{32}S$, $^{34}S/^{32}S$, and $^{36}S/^{32}S$, and some of these provided a qualitative match for the observations from the geologic record. This study recognized that a requirement for the photochemistry seen in these experiments is the presence of ultraviolet radiation with wavelengths shorter than ~280 nm, and that this requirement could be used as a constraint on atmospheric composition. Indeed, several key atmospheric gases absorb at these wavelengths, and this could place upper limits on their abundance. Two gases were examined in this study, ozone and carbon dioxide. By comparing the lifetime for photolysis of sulfur dioxide with its lifetime determined by physical processes (rainout and dry deposition), these workers argued that the amounts of oxygen and carbon dioxide would have to be less than ~0.01–0.002 bar (few percent of present atmospheric level) and ~0.8 bar, respectively. Further experiments are needed, however, and new findings suggest that non-atmospheric reactions may be implicated in some sulfur MIF (e.g., Watanabe et al. 2009).

The experiments by Farquhar et al. (2001) should be considered to be preliminary and it is warranted to provide a small amount of additional discussion of their possible connection to the geologic record. These experiments were undertaken with four different light sources, including two laser sources, and showed coherence between fractionations observed with light sources of similar wavelengths. This coherence was interpreted to suggest a possible dependence of the effects on the wavelength of the ultraviolet radiation. The experiments were not clear analogs of what would happen in the atmosphere and several deficiencies of the experiments are clear, namely that:

- The chemistry in the reaction cells was very complex and included effects associated with many reactions and also shielding of UV within the cells by isotopic species of the reactants and reaction products (self-shielding).
- The experiments done with laser light sources were necessarily of an unrealistically narrow wavelength band which are on the order of that of the fine structure in the absorption spectra of molecules like SO_2, and are not broad enough to capture the spectral shifts due to isotope substitution (e.g., Danielache et al. 2008).
- The experiments done with more intense light sources may have included multiphoton effects—two photons absorbed by one molecule in a shorter time than it can react or relax impart more energy than a single photon and lead to a different outcome.
- The concentrations and number density of sulfur dioxide was much higher than it would be in the atmosphere, leading to the possibility of reaction pathways in the experiments that would not be relevant in the atmosphere.

In spite of these deficiencies, the experiments have been widely cited for identifying a possible candidate for the source of the effect in the Archean samples. This is because the experiments produced large magnitude isotope effects that resemble some of the features seen in the record. However, the types of isotope effects produced by the experiments may have been associated with the primary photolysis reactions, self-shielding, or with secondary reactions that occurred within the cell. These issues however remain unresolved and deserve further investigation.

The experiments of Watanabe et al. (2009) suggest it is possible for nonzero $\Delta^{33}S$ values to be produced by abiotic reduction of sulfate mediated by amino acids, but the origin of the effect seen in these experiments is not clear, and an understanding of the origin turns out to be a critical link in making the case for relevance to the Earth's early sulfur cycle. The experimental results do not provide a clear indication of whether these reactions also produce variations for $\Delta^{36}S$ values by these reactions, and this has implications for the origin of the observed isotope effect. The core issue that needs to be resolved is whether the effect observed by Watanabe et al. (2009) is a kinetic isotope effect of the class referred to as magnetic isotope effects (e.g. Turro 1983; Buchachenko 1995) or whether it is a new type of kinetic isotope effect associated with weak bonding (e.g., Lasaga et al. 2008—but see Balan et al. 2009 for arguments against the existence of this type of effect).

The resolution of this issue may be related to the $\Delta^{36}S$ values of the products of these experiments. It is not possible to rule out an effect on $\Delta^{36}S$ values given the data, but it also is not possible to attribute it to the same step that produced the $\Delta^{33}S$ signal observed in the experiments. It is possible that there is an effect on $\Delta^{33}S$ values which is a magnetic isotope effect that is superimposed on other isotope effects arising from the complex reaction pathways inherent in the experiments. The latter effects would have had an impact on $\Delta^{36}S$ values and further work is therefore needed to address this possibility.

References

Algeo TJ, Lyons TW (2006) Mo-total organic carbon covariation in modern anoxic marine environments: Implications for analysis of paleoredox and paleohydrographic conditions. Paleoceanography 21:PA1016

Anbar AD, Rouxel O (2007) Metal stable isotopes in paleoceanography. Annu Rev Earth Planet Sci 35:717–746

Anbar AD, Duan Y, Lyons TW, Arnold GL, Kendall B, Creaser RA, Kaufman AJ, Gordon GW, Scott C, Garvin J, Buick R (2007) A whiff of oxygen before the Great Oxidation Event? Science 317:1903–1906

Arnold GL, Weyer S, Anbar AD (2004a) Fe isotope variations in natural materials measured using high mass resolution multiple collector ICPMS. Anal Chem 76:322–327

Arnold GL, Anbar AD, Barling J, Lyons TW (2004b) Molybdenum isotope evidence for widespread anoxia in mid-proterozoic oceans. Science 304:87–90

Aspler LB, Chiarenzelli JR, Bursey TL (1994) Ripple marks in quartz arenites of the Hurwitz group, Northwest-territories, Canada—evidence for sedimentation in a vast, early Proterozoic, shallow, fresh-water lake. J Sediment Res Sect A-Sediment Petrol Process 64:282–298

Balan E, Cartigny P, Blanchard M, Cabaret D, Lazzeri M, Mauri F (2009) Theoretical investigation of the anomalous equilibrium fractionation of multiple sulfur isotopes during adsorption. Earth Planet Sci Lett 284:88–93

Barley ME, Pickard AL, Sylvester PJ (1997) Emplacement of a large igneous province as a possible cause of banded iron formation 2.45 billion years ago. Nature 385:55–58

Barley ME, Krapez B, Groves DI, Kerrich R (1998) The Late Archaean bonanza: metallogenic and environmental consequences of the interaction between mantle plumes, lithospheric tectonics, and global cyclicity. Precambrian Research 91:65–90

Beal EJ, House CH, Orphan VJ (2009) Manganese- and iron-dependent marine methane oxidation. Science 325:184–187

Beaumont V, Robert F (1999) Nitrogen isotope ratios of kerogens in Precambrian cherts: a record of the evolution of atmosphere chemistry? Precambr Res 96:63–82

Beaumont VI, Jahnke LL, Des Marais DJ (2000) Nitrogen isotopic fractionation in the synthesis of photosynthetic pigments in Rhodobacter capsulatus and Anabaena cylindrica. Org Geochem 31:1075–1085

Bekker A, Kaufman AJ (2007) Oxidative forcing of global climate change: a biogeochemical record across the oldest Paleoproterozoic ice age in North America. Earth Planet Sci Lett 258: 486–499

Bekker A, Kaufman AJ, Karhu JA, Beukes NJ, Swart QD, Coetzee LL, Eriksson KA (2001) Chemostratigraphy of the Paleoproterozoic Duitschland Formation, South Africa: implications for coupled climate change and carbon cycling. Am J Sci 301:261–285

Bekker A, Holland HD, Wang PL, Rumble D, Stein HJ, Hannah JL, Coetzee LL, Beukes NJ (2004) Dating the rise of atmospheric oxygen. Nature 427:117–120

Bekker A, Kaufman AJ, Karhu JA, Eriksson KA (2005) Evidence for Paleoproterozoic cap carbonates in North America. Precambr Res 137:167–206

Bekker A, Karhu JA, Kaufman AJ (2006) Carbon isotope record for the onset of the Lomagundi carbon isotope excursion in the Great Lakes area, North America. Precambr Res 148: 145–180

Bekker A, Holmden C, Beukes NJ, Kenig F, Eglington B, Patterson WP (2008) Fractionation between inorganic and organic carbon during the Lomagundi (2.22–2.1 Ga) carbon isotope excursion. EPSL 271:278–291

Bekker A, Barley ME, Fiorentini ML, Rouxel OJ, Rumble D, Beresford SW (2009) Atmospheric Sulfur in Archean Komatiite-Hosted Nickel Deposits. Science 326:1086–1089

Bekker A, Slack JF, Planavsky N, Krapež B, Hofmann A, Konhauser KO, Rouxel OJ (2010) Iron formation: the sedimentary product of a complex interplay among mantle, tectonic, oceanic, and biospheric processes. Econ Geol 105:467–508

Bertine KK, Turekian KK (1973) Molybdenum in marine deposits. Geochim Cosmochim Acta 48:605–615

Beukes NJ, Klein C, Kaufman AJ, Hayes JM (1990) Carbonate petrography, kerogen distribution, and carbon and oxygen isotope variations in an early Proterozoic transition from limestone to iron-formation deposition, Transvaal Supergroup, South Africa. Econ Geol Bull Soc Econom Geol 85:663–690

Buchachenko AL (1995) MIE versus CIE—comparative-analysis of magnetic and classical isotope effects. Chem Rev 95:2507–2528

Cameron EM (1982) Sulphate and sulphate reduction in early Precambrian oceans. Nature 296:145–148

Cameron EM (1983) Evidence from early Proterozoic anhydrite for sulfur isotopic partitioning in Precambrian oceans. Nature 304:54–56

Canfield DE (1998) A new model for Proterozoic ocean chemistry. Nature 396:450–453

Canfield DE (2004) The evolution of the Earth surface sulfur reservoir. Am J Sci 304(10):839–861

Canfield DE, Farquhar J (2009) Animal evolution, bioturbation, and the sulfate concentration of the oceans. Proc Acad Sci 106: 8123–8127

Canfield DE, Teske A (1996) Late Proterozoic rise in atmospheric oxygen concentration inferred from phylogenetic and sulphur-isotope studies. Nature 382:127–132

Canfield DE, Habicht KS, Thamdrup B (2000) The Archean sulfur cycle and the early history of atmospheric oxygen. Science 288:658–661

Canfield DE, Poulton SW, Narbonne GM (2007) Late-Neoproterozoic deep-ocean oxygenation and the rise of animal life. Science 315(5808):92–95

Canil D (2002) Vanadium in peridotites, mantle redox and tectonic environments: Archean to present. Earth Planet Sci Lett 195(1–2):75–90

Cao CQ, Love GD, Hays LE, Wang W, Shen SZ, Summons RE (2009) Biogeochemical evidence for euxinic oceans and ecological disturbance presaging the end-Permian mass extinction event. Earth Planet Sci Lett 281:188–201

Carlucci AF, McNally PM (1969) Nitrification by marine bacteria in low concentrations of substrate and oxygen. Limnol Oceanogr 14:736–739

Carpenter EJ, Romans K (1991) Major role of the cyanobacterium Trichodesmium in nutrient cycling in the North-Atlantic Ocean. Science 254:1356–1358

Catling DC (2006) Comment on "A hydrogen-rich early Earth atmosphere". Science 311(5757):38

Catling DC, Claire MW (2005) How Earth's atmosphere evolved to an oxic state: a status report. Earth Planet Sci Lett 237(1–2):1–20

Catling DC, Zahnle KJ, McKay CP (2001) Biogenic methane, hydrogen escape, and the irreversible oxidation of early Earth. Science 293(5531):839–843

Catling DC, Zahnle KJ, McKay CP (2002) What caused the second rise of O_2 in the late Proterozoic?: methane, sulfate, and irreversible oxidation [Abstract: NASA Astrobiology Institute General Meeting]. Astrobiology 2(4):569

Chandler FW (1980) Proterozoic redbed sequences of Canada. Can Geol Surv Bull 311:1–53

Chicarelli MI, Hayes JM, Popp BN, Eckardt CB, Maxwell JR (1993) Carbon and nitrogen isotopic compositions of alkyl porphyrins from the Triassic Serpiano oil-shale. Geochim Cosmochim Acta 57:1307–1311

Claire MW, Catling DC, Zahnle KJ (2006) Biogeochemical modelling of the rise in atmospheric oxygen. Geobiology 4(4):239–269

Cloud PE (1973) Paleoecological significance of the banded iron-formation. Econ Geol 68:1135–1143

Coban-Yildiz Y, Altabet MA, Yilmaz A, Tugrul S (2006) Carbon and nitrogen isotopic ratios of suspended particulate organic matter (SPOM) in the Black Sea water column. Deep-Sea Res II 53: 1875–1892

Coetzee LL (2001) Genetic stratigraphy of the Paleoproterozoic Pretoria Group in the Western Transvaal, MSc. thesis, Rand Afrikaans University, p. 212

Collier RW (1985) Molybdenum in the Northeast Pacific Ocean. Limnol Oceanogr 30:1351–1354

Condie KC, Des Marais DJ, Abbott D (2001) Precambrian superplumes and supercontinents: a record in black shales, carbon isotopes, and paleoclimates? Precambr Res 106:239–260

Czaja AD, Johnson CM, Beard BL, Eigenbrode JL, Freeman KH, Yamaguchi KE (2010) Iron and carbon isotope evidence for ecosystem and environmental diversity in the 2.7 to 2.5 Ga Hamersley Province, Western Australia. Earth Planet Sci Lett 292:170–180

Dalsgaard T, Thamdrup B, Canfield DE (2005) Anaerobic ammonium oxidation (anammox) in the marine environment. Res Microbiol 156:457–464

Danielache SO, Eskebjerg C, Johnson MS, Ueno Y, Yoshida N (2008) High-precision spectroscopy of ^{32}S, ^{33}S, and ^{34}S sulfur dioxide: ultraviolet absorption cross sections and isotope effects. J Geophys Res 113:D17314

Dean DR, Jacobson MR (1992) Biochemical genetics of nitrogenase. In: Stacey G, Burris RH, Evans HJ (eds) Biological Nitrogen Fixation. Chapman and Hall, New York, pp 763–784

Delano JW (2001) Redox history of the Earth's interior since similar to 3900 Ma: implications for prebiotic molecules. Origins Life Evol Biosph 31(4–5):311–341

Delwiche CC, Steyn PL (1970) Nitrogen isotope fractionation in soils and microbial reactions. Environ Sci Technol 4:929–935

Domagal-Goldman SD, Kasting JF, Johnston DT, Farquhar J (2008) Organic haze, glaciations and multiple sulfur isotopes in the Mid-Archean Era. Earth Planet Sci Lett 269:29–40

England GL, Rasmussen B, Krapez B, Groves DI (2002) Paleoenvironmental significance of rounded pyrite in siliciclastic sequences of the Late Archean Witwatersrand Basin: oxygen-deficient atmosphere or hydrothermal alteration? Sedimentology 49:1133–1156

Ettwig KF, Butler MK, Le Paslier D, Pelletier E, Mangenot S, Kuypers MMM, Schreiber F, Dutilh BE, Zedelius J, de Beer D, Gloerich J, Wessels H, van Alen T, Luesken F, Wu ML, van de Pas-Schoonen KT, den Camp H, Janssen-Megens EM, Francoijs KJ, Stunnenberg H, Weissenbach J, Jetten MSM, Strous M (2010) Nitrite-driven anaerobic methane oxidation by oxygenic bacteria. Nature 464:543–548

Farquhar J, Wing BA (2003) Multiple sulfur isotopes and the evolution of the atmosphere. Earth Planet Sci Lett 213:1–13

Farquhar J, Bao HM, Thiemens M (2000) Atmospheric influence of Earth's earliest sulfur cycle. Science 289:756–758

Farquhar J, Savarino J, Airieau S, Thiemens MH (2001) Observation of wavelength-sensitive mass-independent sulfur isotope effects during SO_2 photolysis: implications for the early atmosphere. J Geophys Res-Planet 106:32829–32839

Frank TD, Kah LC, Lyons TW (2003) Changes in organic matter production and accumulation as a mechanism for isotopic evolution in the Mesoproterozoic ocean. Geol Mag 140(4): 397–420

Frei R, Gaucher C, Poulton SW, Canfield DE (2009) Fluctuations in Precambrian atmospheric oxygenation recorded by chromium isotopes. Nature 461:U125–U250

Fry B, Jannasch HW, Molyneaux SJ, Wirsen CO, Muramoto JA, King S (1991) Stable isotope studies of the carbon, nitrogen and sulfur cycles in the Black-Sea and the Cariaco Trench. Deep-Sea Res A 38:S1003–S1019

Garvin J, Buick R, Anbar AD, Arnold GL, Kaufman AJ (2009) Isotopic evidence for an aerobic nitrogen cycle in the latest Archean. Science 323:1045–1048

Gauthier-Lafaye F, Weber F (1989) The Francevillian (Lower Proterozoic) uranium ore deposits of Gabon. Econ Geol 84:2267–2285

Godfrey LV, Falkowski PG (2009) The cycling and redox state of nitrogen in the Archaean ocean. Nature Geoscience 2:725–729

Goldblatt C, Lenton TM, Watson AJ (2006) Bistability of atmospheric oxygen and the Great Oxidation. Nature 443(7112): 683–686

Gross GA (1996) Stratiform iron. In: Eckstrand OR, Sinclair WD, Thorpe RI (eds) Canadian mineral deposit types. Geology of Canada. Geological Survey of Canada, Ottawa, pp 41–80

Grotzinger JP, Kasting JF (1993) New constraints on Precambrian ocean composition. J Geol 101:235–243

Guo QJ, Strauss H, Kaufman AJ, Schroder S, Gutzmer J, Wing B, Baker MA, Bekker A, Jin QS, Kim ST, Farquhar J (2009) Reconstructing Earth's surface oxidation across the Archean-Proterozoic transition. Geology 37:399–402

Habicht KS, Gade M, Thamdrup B, Berg P, Canfield DE (2002) Calibration of sulfate levels in the Archean Ocean. Science 298:2372–2374

Hannah JL, Bekker A, Stein HJ, Markey RJ, Holland HD (2004) Primitive Os and 2316 Ma age for marine shale: implications for Paleoproterozoic glacial events and the rise of atmospheric oxygen. Earth Planet Sci Lett 225:43–52

Harrison AG, Thode HG (1958) Mechanism of the bacterial reduction of sulphate from isotope fractionation studies. Trans Faraday Soc 54:84–92

Hattori K, Campbell FA, Krouse HR (1983a) Sulphur isotope abundances in Aphebian clastic rocks: implications for the coeval atmosphere. Nature 302:323–326

Hattori K, Krouse HR, Campbell FA (1983b) The start of sulphur oxidation in continental environments: about 2.2×10^9 years ago. Science 221:323–326

Hattori K, Campbell FA, Krouse HR (1986) Sulphur isotope abundances in sedimentary rocks, relevance to the evolution of the Precambrian atmosphere. Geochem Int 22:97–115

Hayes JM (1983) Geochemical evidence bearing on the origin of aerobiosis, a seculative hypothesis. In: Schopf JW (ed) The Earth's Earliest Biosphere: Its Origin and Evolution. Princeton University Press, Princeton, NJ, pp 291–301

Hayes JM (1994) Global methanotrophy at the Archean-Proterozoic transition. In: Bengston S (ed) Proceedings of nobel symposium 84, Early Life on Earth. Columbia University Press, New York, pp 220–236

Hayes JM, Waldbauer JR (2006) The carbon cycle and associated redox processes through time. Philos Trans R Soc B 361(1470): 931–950

Heaman LM, Peck D, Toope K (2009) Timing and geochemistry of 1.88 Ga Molson Igneous Events, Manitoba: insights into the formation of a craton-scale magmatic and metallogenic province. Precambr Res 172:143–162

Helz GR, Miller CV, Charnock JM, Mosselmans JFW, Pattrick RAD, Garner CD, Vaughan DJ (1996) Mechanism of molybdenum removal from the sea and its concentration in black shales: EXAFS evidence. Geochim Cosmochim Acta 60:3631–3642

Hinrichs KU (2002) Microbial fixation of methane carbon at 2.7 Ga: was an anaerobic mechanism possible? Geochem Geophys Geosyst 3:10

Hofmann A, Bekker A, Rouxel OJ, Rumble D, Master S (2009) Multiple sulphur and iron isotope composition of detrital pyrite in Archaean sedimentary rocks: a new tool for provenance analysis. Earth Planet Sci Lett 286:436–445

Holland HD (1973) The oceans: a possible source of iron in iron-formations. Econ Geol Bull Soc Econ Geol 68:1169–1172

Holland HD (1984) The chemical evolution of the atmosphere and oceans. Princeton University Press, Princeton

Holland HD (2002) Volcanic gases, black smokers, and the Great Oxidation Event. Geochim Cosmochim Acta 66:3811–3826

Holland HD (2003) Discussion of the article by A. C. Lasaga and H. Ohmoto on "The oxygen geochemical cycle: dynamics and stability," Geochim. Cosmochim. Acta 66, 361–381, 2002. Geochim Cosmochim Acta 67:787–789

Holland HD (2004) The geological history of seawater. In: Holland HD, Turekian KK (eds) Treatise on geochemistry. Elsevier, Oxford, pp 583–625

Holland HD (2005) Sedimentary mineral deposits and evolution of Earth's near surface environments. Econ Geol 100:1489–1509

Holland HD (2006) The oxygenation of the atmosphere and oceans. Philos Trans R Soc B 361:903–915

Holland HD (2009) Why the atmosphere became oxygenated: a proposal. Geochim Cosmochim Acta 73:5241–5255

Isley AE (1995) Hydrothermal plumes and the delivery of iron to banded iron-formation. J Geol 103:169–185

Isley AE, Abbott DH (1999) Plume-related mafic volcanism and the deposition of banded iron formation. J Geophys Res Solid Earth 104:15461–15477

Jia YF (2006) Nitrogen isotope fractionations during progressive metamorphism: a case study from the Paleozoic Cooma metasedimentary complex, southeastern Australia. Geochim Cosmochim Acta 70:5201–5214

Jia YF, Kerrich R (2004) Nitrogen 15-enriched Precambrian kerogen and hydrothermal systems. Geochem Geophys Geosyst 5:Q07 005

Jiang S-Y, Chen Y-Q, Ling H-F, Yang J-H, Feng H-Z, Ni P (2006) Trace- and rare-earth element geochemistry and Pb-Pb dating of black shales and intercalated Ni-Mo-PGE-Au sulfide ores in Lower Cambrian strata, Yangtze Platform, South China. Miner Depos 41:453–467

Joachimski MM, Ostertag-Hennig C, Pancost RD, Strauss H, Freeman KH, Littke R, Sinninghe Damste JS, Racki G (2001) Water column anoxia, enhanced productivity and concomitant changes in δ^{13}C and $\delta\ ^{34}$S across the Frasnian-Famennian boundary (Kowala-Holy Cross Mountains/Poland). Chem Geol 175:109–131

Johnson CM, Beard BL, Roden EE (2008) The iron isotope fingerprints of redox and biogeochemical cycling in the modern and ancient. Earth Ann Rev Earth Planet Sci. 36:457–493

Johnston DT, Wing BA, Farquhar J, Kaufman AJ, Strauss H, Lyons TW, Kah LC, Canfield DE (2005) Active microbial sulfur disproportionation in the Mesoproterozoic. Science 310(5753): 1477–1479

Junium CK, Arthur MA (2007) Nitrogen cycling during the cretaceous, Cenomanian-Turonian oceanic anoxic event II. Geochem Geophys Geosyst 8:Q03002

Kah LC, Lyons TW, Frank TD (2004) Low marine sulphate and protracted oxygenation of the proterozoic biosphere. Nature 431(7010):834–838

Karhu JA, Holland HD (1996) Carbon isotopes and the rise of atmospheric oxygen. Geology 24:867–870

Kashiyama Y, Ogawa NO, Kuroda J, Shiro M, Nomoto S, Tada R, Kitazato H, Ohkouchi N (2008) Diazotrophic cyanobacteria as the major photoautotrophs during mid-Cretaceous oceanic anoxic events: nitrogen and carbon isotopic evidence from sedimentary porphyrin. Org Geochem 39:532–549

Kasting JF (1993) Earths early atmosphere. Science 259(5097): 920–926

Kasting JF (2001) Earth history—the rise of atmospheric oxygen. Science 293:819–820

Kasting JF, Siefert JL (2001) The nitrogen fix. Nature 412:26–27

Kaufman AJ, Knoll AH (1995) Neoproterozoic variations in the C-isotopic composition of seawater—stratigraphic and biogeochemical implications. Precambrian Res 73:27–49

Kaufman AJ, Johnston DT, Farquhar J, Masterson AL, Lyons TW, Bates S, Anbar AD, Arnold GL, Garvin J, Buick R (2007) Late Archean biospheric oxygenation and atmospheric evolution. Science 317:1900–1903

Kendall B, Reinhard CT, Lyons TW, Kaufman AJ, Poulton SW, Anbar AD (2010) Pervasive oxygenation along late Archaean ocean margins: Nat Geosci 3:647–652

Kirkham RV, Roscoe SM (1993) Atmospheric evolution and ore deposit formation. Resource Geology Special Issue 15:1–17

Kirschvink JL, Kopp RE (2008) Palaeoproterozoic ice houses and the evolution of oxygen-mediating enzymes: the case for a late origin of photosystem II. Philos Trans R Soc B 363(1504): 2755–2765

Konhauser KO, Newman DK, Kappler A (2005) The potential significance of microbial Fe(III) reduction during deposition of Precambrian banded iron formations. Geobiology 3:167–177

Konhauser KO, Pecoits E, Lalonde SV, Papineau D, Nisbet EG, Barley ME, Arndt NT, Zahnle K, Kamber BS (2009) Oceanic nickel depletion and a methanogen famine before the Great Oxidation Event. Nature 458:750–U785

Kopp RE, Kirschvink JL, Hilburn IA, Nash CZ (2005) The paleoproterozoic snowball Earth: a climate disaster triggered by the evolution of oxygenic photosynthesis. Proc Natl Acad Sci USA 102(32):11131–11136

Kulikov YN, Lammer H, Lichtenegger HIM, Penz T, Breuer D, Spohn T, Lundin R, Biernat HK (2007) A comparative study of the influence of the active young sun on the early atmospheres of earth, venus, and mars. Space Sci Rev 129(1–3):207–243

Kump LR, Barley ME (2007) Increased subaerial volcanism and the rise of atmospheric oxygen 2.5 billion years ago. Nature 448: 1033–1036

Kump LR, Brantley SL, Arthur MA (2000) Chemical, weathering, atmospheric CO_2, and climate. Annu Rev Earth Planet Sci 28:611–667

Kuypers MMM, van Breugel Y, Schouten S, Erba E, Sinninghe Damste JS (2004) N_2-fixing cyanobacteria supplied nutrient N for Cretaceous oceanic anoxic events. Geology 32:853–856

Lam P, Lavik G, Jensen MM, van de Vossenberg J, Schmid M, Woebken D, Dimitri G, Amann R, Jetten MSM, Kuypers MMM (2009) Revising the nitrogen cycle in the Peruvian oxygen minimum zone. Proc Natl Acad Sci USA 106:4752–4757

Lasaga AC, Otake T, Watanabe Y, Ohmoto H (2008) Anomalous fractionation of sulfur isotopes during heterogeneous reactions. Earth Planet Sci Lett 268:225–238

Lecuyer C, Ricard Y (1999) Long-term fluxes and budget of ferric iron: implication for the redox states of the Earth's mantle and atmosphere. Earth Planet Sci Lett 165:197–211

Li ZXA, Lee CTA (2004) The constancy of upper mantle fO(2) through time inferred from V/Sc ratios in basalts. Earth Planet Sci Lett 228(3–4):483–493

Lindstrom ES, Tove SR, Wilson PW (1950) Nitrogen fixation by the green and purple sulfur bacteria. Science 112:197–198

Logan GA, Hayes JM, Hieshima GB, Summons RE (1995) Terminal Proterozoic reorganization of biogeochemical cycles. Nature 376:53–56

Lyons TW, Werne JP, Hollander DJ, Murray RW (2003) Contrasting sulfur geochemistry and Fe/Al and Mo/Al ratios across the last oxic-to-anoxic transition in the Cariaco Basin, Venezuela. Chem Geol 195:131–157

MacGregor AM (1927) The problem of the Precambrian atmosphere. S Afr J Sci 24:155–172

McManus J, Nägler TF, Siebert C, Wheat CG, Hammond DE (2002) Oceanic molybdenum isotope fractionation: diagenesis and hydrothermal ridge-flank alteration. Geochem Geophys Geosys 3:9

McManus J, Berelson WM, Severmann S, Poulson RL, Hammond DE, Klinkhammer GP, Holm C (2006) Molybdenum and uranium geochemistry in continental margin sediments: paleoproxy potential. Geochim Cosmochim Acta 70:4643–4662

Melezhik VA, Fallick AE, Medvedev PV, Makarikhin VV (1999) Extreme ^{13}C(carb) enrichment in ca, 2.0 Ga magnesite-stromatolite-dolomite- 'red beds' association in a global context: a case for the world-wide signal enhanced by a local environment. Earth Sci Rev 48:71–120

Melezhik VA, Fallick AE, Hanski EJ, Kump LR, Lepland A, Prave AR, Strauss H (2005) Emergence of the aerobic biosphere during the Archean-Proterozoic transition: challenges of future research today. GSA Today 15:4–11

Miyake Y, Wada E (1971) The isotope effect on the nitrogen in biochemical, oxidation-reduction reactions. Recent Oceanogr Works Jpn 11:1–6

Monster J, Appel PWU, Thode HG, Schidlowski M, Carmichael CM, Bridgwater D (1979) Sulfur isotope studies in early Archaean sediments from Isua, West Greenland—implications for the antiquity of bacterial sulfate reduction. Geochim Cosmochim Acta 43:405–413

Morford JL, Emerson SS (1999) The geochemistry of redox sensitive trace metals in sediments. Geochim Cosmochim Acta 63: 1735–1750

Navarro-Gonzalez R, McKay CP, Mvondo DN (2001) A possible nitrogen crisis for Archaean life due to reduced nitrogen fixation by lightning. Nature 412:61–64

Ohkouchi N, Nakajima Y, Okada H, Ogawa NO, Suga H, Oguri K, Kitazato H (2005) Biogeochemical processes in the saline meromictic Lake Kaiike, Japan: implications from molecular isotopic evidences of photosynthetic pigments. Environ Microbiol 7:1009–1016

Ohkouchi N, Kashiyama Y, Kuroda J, Ogawa NO, Kitazato H (2006) The importance of diazotrophic cyanobacteria as primary producers during Cretaceous Oceanic Anoxic Event 2. Biogeosciences 3:467–478

Ono S, Eigenbrode JL, Pavlov AA, Kharecha P, Rumble D, Kasting JF, Freeman KH (2003) New insights into Archean sulfur cycle from mass-independent sulfur isotope records from the Hamersley Basin, Australia. Earth Planet Sci Lett 213:15–30

Ono S, Beukes NJ, Rumble DI (2009a) Origin of two distinct multiple-sulfur isotope compositions of pyrite in the 2.5 Ga Klein Naute Formation, Griqualand West Basin, South Africa. Precambr Res 169:48–57

Ono S, Kaufman AJ, Farquhar J, Sumner DY, Beukes NJ (2009b) Lithofacies control on multiple-sulfur isotope records and Neoarchean sulfur cycles. Precambr Res 169:58–67

Panahi A, Young GM, Rainbird RH (2000) Behaviour of major and trace elements (including REE) during the Paleoproterozoic pedogenesis and diagenetic alteration of an Archean granite near Ville Marie, Quebec, Canada. Geochim Cosmochim Acta 64:2199–2220

Pancost RD, Crawford N, Magness S, Turner A, Jenkyns H, Maxwell JR (2004) Further evidence for the development of photic-zone euxinic conditions during Mesozoic oceanic anoxic events. Geol Soc (Lond) J 161:353–364

Papineau D, Mojzsis SJ, Karhu JA, Marty B (2005) Nitrogen isotopic composition of ammoniated phyllosilicates: case studies from Precambrian metamorphosed sedimentary rocks. Chem Geol 216:37–58

Papineau D, Mojzsis SJ, Schmitt AK (2007) Multiple sulfur isotopes from Paleoproterozoic Huronian interglacial sediments and the rise of atmospheric oxygen. Earth Planet Sci Lett 255: 188–212

Papineau D, Purohit R, Goldberg T, Pi DH, Shields GA, Bhu H, Steele A, Fogel ML (2009) High primary productivity and nitrogen cycling after the Paleoproterozoic phosphogenic event in the Aravalli Supergroup, India. Precambr Res 171:37–56

Partin C, Bekker A, Scott C, Gill B, Lyons T (2010) Uranium in shales as a proxy for the evolution of surficial redox conditions. GeoCanada 2010: Abstract

Pavlov AA, Kasting JF (2002) Mass-independent fractionation of sulfur isotopes in Archean sediments: strong evidence for an anoxic Archean atmosphere. Astrobiology 2:27–41

Pavlov AA, Kasting JF, Eigenbrode JL, Freeman KH (2001) Organic haze in Earth's early atmosphere: Source of low-C-13 Late Archean kerogens? Geology 29:1003–1006

Perry EC, Monster J, Reimer TO (1971) Sulfur isotopes in Swaziland System barite and the evolution of Earth's atmosphere. Science 171:1015–1016

Peter JM, Goodfellow WD, Doherty W (2003) Hydrothermal sedimentary rocks of the Heath Steele Belt, Bathurst Mining Camp, New Brunswick: part 2, bulk and rare earth element geochemistry and implications for origin. Econ Geol Monogr 11:391–415

Peters KE, Sweeney RE, Kaplan IR (1978) Correlation of carbon and nitrogen stable isotope ratios in sedimentary organic matter. Limnol Oceanogr 23:598–604

Pinti DL, Hashizume K (2001) ^{15}N-depleted nitrogen in Early Archean kerogens: clues on ancient marine chemosynthetic-based ecosystems? A comment to Beaumont, V., Robert, F., 1999. Precambrian Res. 96, 62–82. Precambrian Research 105:85–88

Pinti DL, Hashizume K, Sugihara A, Massault M, Philippot P (2009) Isotopic fractionation of nitrogen and carbon in Paleoarchean cherts from Pilbara craton, Western Australia: Origin of N-15-depleted nitrogen. Geochim Cosmochim Acta 73:3819–3848

Planavsky N, Rouxel OJ, Bekker A, Shapiro R, Fralick PW, Knudsen A (2009) Iron-oxidizing microbial ecosystems thrived in late Paleoproterozoic redox-stratified oceans. Earth Planet Sci Lett 286:230–242

Pope MC, Grotzinger JP (2003) Paleoproterozoic stark formation, Athapuscow Basin, Northwest Canada: record of cratonic-scale salinity crisis. J Sediment Res 73:280–295

Poulton SW, Raiswell R (2002) The low-temperature geochemical cycle of iron: from continental fluxes to marine sediment deposition. Am J Sci 302:774–805

Poulton SW, Krom MD, Raiswell R (2004) A revised scheme for the reactivity of iron (oxyhydr)oxide minerals towards dissolved sulfide. Geochim Cosmochim Acta 68:3703–3715

Poulton SW, Bekker A, Canfield DE (2009) Early Paleoproterozoic fluctuations in biospheric oxygenation. Geochim Cosmochim Acta 73:A1047–A1047

Prasad N, Roscoe SM (1996) Evidence of anoxic to oxic atmosphere change during 2.45–2.22 Ga from lower and upper sub-Huronian paleosols, Canada. Catena 27:105–121

Rainbird RH, Nesbitt HW, Donaldson JA (1990) Formation and diagenesis of a sub-Huronian saprolith: comparison with a modern weathering profile. J Geol 98:801–822

Rasmussen B, Buick R (1999) Redox state of the Archean atmosphere: evidence from detrital heavy minerals in ca. 3250–2750 Ma sandstones from the Pilbara Craton, Australia. Geology 27:115–118

Rasmussen B, Fletcher IR, Brocks JJ, Kilburn MR (2008) Reassessing the first appearance of eukaryotes and cyanobacteria. Nature 455:1101–1104

Rees CE (1973) Steady-state model for sulfur isotope fractionation in bacterial reduction processes. Geochim Cosmochim Acta 37:1141–1162

Reinhard CT, Raiswell R, Scott C, Anbar AD, Lyons TW (2009) A late Archean sulfidic sea stimulated by early oxidative weathering of the continents. Science 326:713–716

Roscoe SM (1996) Paleoplacer uranium gold. In: Eckstrand OR, Sinclair WD, Thorpe RI (eds) Geology of Canadian mineral deposit types, vol P-1. Geological Society of America, The Geology of North America, Boulder, pp 10–23

Rouxel OJ, Bekker A, Edwards KJ (2005) Iron isotope constraints on the Archean and Paleoproterozoic ocean redox state. Science 307:1088–1091

Rye R, Holland HD (1998) Paleosols and the evolution of atmospheric oxygen: a critical review. Am J Sci 298:621–672

Sachs JP, Repeta DJ (1999) Oligotrophy and nitrogen fixation during eastern Mediterranean sapropel events. Science 286:2485–2488

Sachs JP, Repeta DJ, Goericke R (1999) Nitrogen and carbon isotopic ratios of chlorophyll from marine phytoplankton. Geochim Cosmochim Acta 63:1431–1441

Schidlowski M (1966) Beiträge zur Kenntnis der radioactiven Bestandteile der Witwatersrand-Konglomerate. I Uranpecherz in den Konglomeraten des Oranje-Freistaat-Goldfeldes. Neues Jahrbuch für Mineralogie Abhandlungen 105:183–202

Schröder S, Bekker A, Beukes NJ, Strauss H, van Niekerk HS (2008) Rise in seawater sulphate concentration associated with the Paleoproterozoic positive carbon isotope excursion: evidence from sulphate evaporites in the 2.2–2.1 Gyr shallow-marine Lucknow Formation, South Africa. Terra Nova 20:108–117

Schrum HN, Spivack AJ, Kastner M, D'Hondt S (2009) Sulfate-reducing ammonium oxidation: a thermodynamically feasible metabolic pathway in subseafloor sediment. Geology 37: 939–942

Scott C, Lyons TW, Bekker A, Shen Y, Poulton SW, Chu X, Anbar A (2008) Tracing the stepwise oxygenation of the Proterozoic ocean. Nature 452:456–460

Sessions AL, Doughty DM, Welander PV, Summons RE, Newman DK (2009) The continuing puzzle of the Great Oxidation Event. Curr Biol 19:R567–R574

Shen Y, Farquhar J, Masterson AM, Kaufman AJ, Buick R (2009) Evaluating the role of microbial sulfate reduction in the early Archean using quadruple isotope systematics. Earth Planet Sci Lett 279:383–391

Sinninghe Damste JS, Koester J (1998) A euxinic southern North Atlantic Ocean during the Cenomanian Turonian oceanic anoxic event. Earth Planet Sci Lett 158:165–173

Slack JF, Cannon WF (2009) Extraterrestrial demise of banded iron formations 1.85 billion years ago. Geology 37:1011–1014

Slack JF, Grenne T, Bekker A, Rouxel OJ, Lindberg PA (2007) Suboxic deep seawater in the late Paleoproterozoic: evidence from hematitic chert and iron formation related to seafloor-hydrothermal sulfide deposits, central Arizona, USA. Earth Planet Sci Lett 255:243–256

Sleep NH, Bird DK (2008) Evolutionary ecology during the rise of dioxygen in the Earth's atmosphere. Philos Trans R Soc B 363(1504):2651–2664

Sweeney RE, Liu KK, Kaplan IR (1978) Oceanic nitrogen isotopes and their uses in determining the source of sedimentary nitrogen. In: Robinson BW (ed) Stable Isotopes in the Earth Sciences, vol 220. DSIR Bulletin, Wellington, pp 9–26

Taylor SR, McLennan SM (1995) The geochemical evolution of the continental crust. Reviews in Geophysics 33:241–265

Thode HG, Macnamara J, Collins CB (1949) Natural variations in the isotopic content of sulphur and their significance. Can J Res B 27:361–373

Tian F, Toon OB, Pavlov AA, De Sterck H (2005) A hydrogen-rich early Earth atmosphere. Science 308(5724):1014–1017

Tian F, Solomon SC, Qian LY, Lei JH, Roble RG (2008) Hydrodynamic planetary thermosphere model: 2. Coupling of an electron transport/energy deposition model. J Geophys Res-Planet 113(E7)

Tsikos H, Moore JM (1997) Petrography and geochemistry of the Paleoproterozoic Hotazel Iron-Formation, Kalahari Manganese Field, South Africa: Implications for Precambrian Manganes Metallogenesis. Econ Geol 92:87–97

Turro NJ (1983) Influence of nuclear-spin on chemical-reactions—magnetic isotope and magnetic-field effects (a review). Proc Natl Acad Sci USA 80:609–621

Ueno Y, Johnson MS, Danielache SO, Eskebjerg C, Pandey A, Yoshida N (2009) Geological sulfur isotopes indicate elevated OCS in the Archean atmosphere, solving faint young sun paradox. Proc Natl Acad Sci USA 106:14784–14789

Voss M, Nausch G, Montoya JP (1997) Nitrogen stable isotope dynamics in the central Baltic Sea: influence of deep-water renewal on the N-cycle changes. Mar Ecol Prog Ser 158:11–21

Wahlund TM, Madigan MT (1993) Nitrogen-fixation by the thermophilic green sulfur bacterium Chlorobium tepidum. J Bacteriol 175:81–90

Watanabe Y, Farquhar J, Ohmoto H (2009) Anomalous fractionations of sulfur isotopes during thermochemical sulfate reduction. Science 324:370–373

Wellman RP, Cook FD, Krouse HR (1968) Nitrogen-15: microbiological alteration of abundance. Science 161:269–270

Wille M, Kramers JD, Nagler TF, Beukes NJ, Schroder S, Meisel T, Lacassie JP, Voegelin AR (2007) Evidence for a gradual rise of oxygen between 2.6 and 2.5 Ga from Mo isotopes and Re-PGE signatures in shales. Geochim Cosmochim Acta 71:2417–2435

Wood J (1973) Stratigraphy and depositional environments of upper Huronian rocks of the Rawhide Lake-Flack Lake area, Ontario. In: Young GM (ed) Huronian Stratigraphy and Sedimentation, vol 12. Geological Association of Canada Special Paper, Geological Association of Canada, pp 73–95

Yamaguchi KE (2002) Geochemistry of Archean-Paleoproterozoic black shales: early evolution of the atmosphere, oceans, and biosphere, Ph.D. dissertation, Department of Geosciences, Pennsylvania State University, 456 pp

Yamaguchi KE, Ohmoto H (2006) Comment on "Iron isotope constraints on the Archean and Paleoproterozoic ocean redox state". Science 311:177a

Yamaguchi KE, Johnson CM, Beard BL, Ohmoto H (2005) Biogeochemical cycling of iron in the Archean-Paleoproterozoic Earth: constraints from iron isotope variations in sedimentary rocks from the Kaapvaal and Pilbara Cratons. Chem Geol 218:135–169

Yang W, Holland HD (2002) The redox-sensitive trace elements, Mo, U, and Re in Precambrian carbonaceous shales: indicators of the Great Oxidation Event. GSA Abstr Progr 34:381

Yang W, Holland HD (2003) The Hekpoort paleosol profile in Strata 1 at Gaborone, Botswana: soil formation during the great oxidation event. Am J Sci 303:187–220

Zahnle K, Claire M, Catling D (2006) The loss of mass-independent fractionation in sulfur due to a Palaeoproterozoic collapse of atmospheric methane. Geobiology 4(4):271–283

Zerkle AL, Junium CK, Canfield DE, House CH (2008) Production of ^{15}N-depleted biomass during cyanobacterial N_2-fixation at high Fe concentrations. J Geophys Res 113:G03014